Modeling and Mechanistic Investigation of α-synuclein aggregation

Svanbergsson, Alexander

2021

Document Version:
Publisher's PDF, also known as Version of record

Modeling and Mechanistic Investigation of α-Synuclein Aggregation

ALEXANDER SVANBERGSSON
DEPARTMENT OF EXPERIMENTAL MEDICAL SCIENCE | LUND UNIVERSITY

Printed by Media-Tryck, Lund 2021 NORDIC SWAN ECOLABEL 3041 0903

LUND UNIVERSITY

FACULTY OF MEDICINE

Department of Experimental Medical Science

Lund University, Faculty of Medicine
Doctoral Dissertation Series 2021:136
ISBN 978-91-8021-143-7
ISSN 1652-8220

Modeling and Mechanistic Investigation of α-Synuclein Aggregation

Alexander Svanbergsson

LUND
UNIVERSITY

DOCTORAL DISSERTATION

By due permission of the Faculty of Medicine at Lund University
this thesis will be defended on December 3rd, 2021 at 13:15
in Belfragesalen, BMC D15 klinikgatan 32, Lund, Sweden

FACULTY OPPONENT

Kelvin C. Luk

Stem cells and Neurogenesis Unit
Perelman School of Medicine
Philadelphia, PA, United States

Organization LUND UNIVERSITY Molecular Neuromodulation Department of experimental medical sciences Faculty of medicine, Lund University	Document name DOCTORAL DISSERTATION
	Date of issue December 3rd, 2021
Author(s) Alexander Svanbergsson	Sponsoring organization

Title and subtitle
Modeling and Mechanistic Investigation of α-synuclein Aggregation

Abstract

Our understanding of the α-synuclein aggregation process and the consequences thereof is currently limited, which in turn prevents the development of targeted therapeutic interventions. The work presented here, as a part of this thesis, is focused on expanding our understanding of the molecular events involved in α-synuclein aggregation. Towards this goal we have studied the impact of pathologically relevant forms of α-synuclein, namely A53T mutant α-synuclein and fibrillar α-synuclein, and characterized their impact on N-methyl-D-aspartate receptor (NMDAR) diffusion and function. We found both mutant and fibrillar α-synuclein, decreased the NMDAR diffusion and expression at the post-synapse. Moving further towards the mechanistic investigations we investigated the effect of two neuroprotective compounds on α-synuclein aggregation and found both compounds capable of clearing α-synuclein in cell and animal models potentially through autophagy related functions. In our efforts to scale mechanistic investigations we developed a high-throughput screening (HTS) capable FRET-based reporter for detection of α-synuclein aggregation in cells. Using this model, we performed a proof-of-concept screen of kinase inhibitors from which we identified three inhibitors with potent protective effects on α-synuclein aggregation. We further showed through mechanistic investigation that the protective effects likely involved lysosomal changes. Finally, in an effort to advance our knowledge of α-synuclein aggregation, we performed a genome-wide knockout screen to identify genes in the human genome with an impact on α-synuclein aggregation. This study also highlighted among other pathways the importance of the endolysosomal system in relation to α-synuclein aggregation. Many questions remain in regard to the molecular mechanisms involved in α-synuclein aggregation, but we hope our insights and models presented here will assist in the elucidation of the underlying mechanisms of α-synuclein aggregation.

Key words: Synucleinopathy, Parkinson´s disease, dementia with Lewy bodies, Multiple system atrophy, Mechanistic, modeling, alpha-synuclein, CRISPR, PKC, p38 MAPK

Classification system and/or index terms (if any)

Supplementary bibliographical information		Language: English
ISSN and key title 1652-8220		ISBN 978-91-8021-143-7
Recipient's notes	Number of pages: 81	Price
	Security classification	

Signature  Date 2021-11-04

Modeling and Mechanistic Investigation of α-Synuclein Aggregation

by

Alexander Svanbergsson

from

NEURAL PLASTICITY & REPAIR

Department of Experimental Medical Science, Faculty of Medicine

Lund University, Lund, Sweden

FACULTY OF MEDICINE

Cover by Matilde Negrini & Maria Rodriguez Zabala

Faculty of Medicine
Department of Experimental Medical Science

ISBN 978-91-8021-143-7
ISSN 1652-8220
Lund University, Faculty of Medicine Doctoral Dissertation Series 2021:136

Printed in Sweden by Media-Tryck, Lund University
Lund 2021

To my family,
for always being there when i have needed you

The most important step a person can take
is the next one"
-Brandon Sanderson

"Make haste slowly"
-Emperor Augustus

Table of contents

Original papers and manuscripts included in the thesis

I. Wu J-Z, Ardah M, Haikal C, **Svanbergsson A**, Diepenbroek M, Vaikath N N, Li W, Wang Z-Y, Outeiro T F, El-Agnaf O M and Li J-Y 2019 Dihydromyricetin and Salvianolic acid B inhibit α-synuclein aggregation and enhance chaperone-mediated autophagy Transl Neurodegener 8 18

II. Huang T T, Gou D H, **Svanbergsson A**, Li W, Li J-Y * and Groc L* Pathological α-synuclein triggers synaptic NMDA receptor dysfunction through altered trafficking. (Manuscript in preparation) (* Senior authors)

III. **Svanbergsson A**, Ek F, Martinsson I, Rodo J, Liu D, Brandi E, Haikal C, Torres-Garcia L, Li W, Gouras G, Olsson R, Björklund T and Li J-Y 2021 FRET-Based Screening Identifies p38 MAPK and PKC Inhibition as Targets for Prevention of Seeded α-Synuclein Aggregation Neurotherapeutics 1–18

IV. **Svanbergsson A**, Davidsson M, Rodriguez-Zabala M, Järås M, Björklund T, Li J-Y Genome-wide screening for the identification of genetic modifiers of α-synuclein aggregation. (Manuscript in preparation)

Published papers and manuscripts outside of the thesis

V Paulus A, Engdahl A, Yang Y, Boza-Serrano A, Bachiller S, Torres-Garcia L, **Svanbergsson A**, Garcia M G, Gouras G K, Li J-Y, Deierborg T and Klementieva O 2021 Amyloid Structural Changes Studied by Infrared Microspectroscopy in Bigenic Cellular Models of Alzheimer's Disease Int J Mol Sci 22 3430

VI. Davidsson M, Negrini M, Hauser S, **Svanbergsson A**, Lockowandt M, Tomasello G, Manfredsson F P and Heuer A 2020 A comparison of AAV-vector production methods for gene therapy and preclinical assessment Sci Rep-uk 10 21532

VII. Zhong C-B, Chen Q-Q, Haikal C, Li W, **Svanbergsson A**, Diepenbroek M and Li J-Y 2017 Age-Dependent α-Synuclein Accumulation and Phosphorylation in the Enteric Nervous System in a Transgenic Mouse Model of Parkinson's Disease Neurosci Bull 33 483–92

VIII. Liu D, Guo J-J, Su J-H, **Svanbergsson A**, Yuan L, Haikal C, Li W, Gouras G and Li J-Y 2021 Differential seeding and propagating efficiency of α-synuclein strains generated in different conditions Transl Neurodegener 10 20

IX. Haikal C, Ortigosa-Pascual L, Najarzadeh Z, Bernfur K, **Svanbergsson A**, Otzen D E, Linse S and Li J-Y 2021 The Bacterial Amyloids Phenol Soluble Modulins from Staphylococcus aureus Catalyze α-Synuclein Aggregation Int J Mol Sci 22 11594

X. Martinsson I, Quintino L, Garcia M, **Svanbergsson A**, Strange O, England R, Li J-Y, Lundberg C, Gouras G K 2021 Alzheimer's Aβ-induced hyper-excitability implicates dysregulation of homeostatic synaptic plasticity. (Manuscript in preparation)

XI. Torres-Garcia L, Domingues M P J, Brandi E, Haikal C, Brás C I, Gerhardt E, Li W, **Svanbergsson A**, Outeiro T F, Gouras G K, Li J-Y 2021 Monitoring α-synuclein – Tau interactions *in vitro* and *in vivo* using bimolecular fluorescence complementation. (Submitted for publication)

Summary

As the idiom goes “with age comes wisdom”, but sadly it also comes with increased risk of developing neurodegenerative disorders. Age is the primary risk factor for many such diseases, though it also depends on genetic predisposition.

Synucleinopathies are a subset of these, including Parkinson’s disease (PD), Dementia with Lewy bodies (DLB) and Multiple system atrophy (MSA). These varied neurodegenerative diseases progress in an irreversible manner and are associated with severe symptoms including dementia, rigidity, postural instability, shaking or cognitive impairment depending on the disease.

Currently, the mainstay treatment for synucleinopathies focuses on relieving the symptoms and improving quality of life for affected patients. This is achieved with symptomatic treatments, such as dopamine replacement therapy with levodopa for patients with PD. This first line treatment has remained relatively unchanged for 40 years, given the lack of curative treatment options. This stems in part from our lacking understanding of the underlying principles of disease progression. It has been shown that misfolding of the neuronal protein α-synuclein accumulates in Lewy bodies and constitutes a pathogenic hallmark of all synucleinopathies. Despite the partly causative role of α-synuclein aggregation in pathology, our understanding of its involvement is currently lacking.

The work presented as a part of this thesis is focused on the development of new sensitive methods to study α-synuclein and its role in neurodegeneration. We show how modeling inheritable PD-associated mutations in the α-synuclein gene (*SNCA*) can lead to disease-associated changes in neurons, and that misfolded α-synuclein can impose similar effects.

By combining these different α-synuclein-based models, we recapitulate several cardinal features of PD pathology. This makes it an attractive experimental model for studies aimed at identifying neuroprotective compounds and characterising how this disease modification occurs. With the work reported in this thesis, we hope to provide new insights into α-synuclein aggregation that may contribute to the development of new and potentially disease-modifying treatments for synucleinopathies.

Populärvetenskaplig sammanfattning

Som uttrycket säger “med åldern kommer vishet”, men tyvärr kommer det också med ökad risk att utveckla neurodegenerativa sjukdomar. Ålder är den största riskfaktorn för många sådana sjukdomar, även om det också kan bero på genetiska faktorer.

Synukleinopatier är en undergrupp av neurodegenerativa sjukdomar som inkluderar Parkinsons sjukdom (PS), Lewy body demens och multipel systematrofi. Dessa sjukdomar utvecklas på ett irreversibelt sätt och är förknippade med allvarliga symtom som demens, stelhet, postural instabilitet, skakningar och kognitiv nedsättning.

För närvarande inriktas behandlingen av synukleinopatier på att lindra symtomen och förbättra livskvaliteten för de drabbade patienterna. Detta uppnås med symtomatiska behandlingar, såsom dopaminersättningsterapi med levodopa för patienter med PS. Denna behandling har varit relativt oförändrad i 40 år, mycket beroende på att det saknas behandlingsalternativ för att bota sjukdomen. Detta beror delvis på vår bristande förståelse för de underliggande principerna för sjukdomsförloppen. Proteinet α-synuklein, som finns i cellerna i hjärnan, har visat sig spela en viktig roll i sjukdomsförloppen, men exakt hur proteinet gör det är okänt.

För att utveckla bättre behandlingsalternativ måste vi bygga en bättre förståelse för de händelser som leder fram till sjukdomarna. Med sådan kunskap kan behandlingar som riktar sig till tidiga stadier av sjukdomarna utvecklas.

Arbetet som presenteras i denna avhandling är fokuserat på att utveckla nya och känsligare metoder för att studera α-synuklein och dess roll i neurodegeneration. I avhandlingen visar vi hur modellering av ärftliga mutationer i genen som kodar för α-synuklein kan leda till sjukdomsassocierade förändringar i nervceller och att felveckat α-synuklein kan åstadkomma liknande effekter.

Genom att kombinera dessa olika α-synukleinbaserade modeller har vi kunnat utveckla modellsystem som efterliknar delar av sjukdomspatologin, nämligen aggregeringen av α-synuklein. I syfte att bättre förstå vad som händer under sjukdomsförloppet har vi undersökt preparat som skulle kunna ha terapeutisk effekt på aggregering av α-synuklein. Genom våra experiment hittade vi tre preparat som minskade den sjukdomsrelaterade aggregeringen. Hur, och om, dessa preparat skulle kunna användas som behandlingar är ännu inte fastställt, men våra experiment visar att vårt modellsystem kan hjälpa till att identifiera nya behandlingar för

att förhindra aggregering av α-synuklein.

Förutom att undersöka enskilda preparat använder vi också denna modell för att undersöka effekten som någon av de 19050 gener från det mänskliga genomet har på processen för a-synukleinaggregering.

Genom att bygga en förståelse för vad som händer med α-synuklein hoppas vi kuna bidra till utvecklingen av nya och potentiellt sjukdomsmodifierande behandlingar för synukleinopatier.

Abbreviations

6-OHDA	6-Hydroxydopamine
AD	Alzheimer's disease
BAC	Bacterial Artificial Chromosome
BSE	Bovine spongiform encephalopathy
CBD	Corticobasal degeneration
CFP	Cyan fluorescent protein
CJD	Creutzfeldt-Jacobs disease
CMA	Chaperone-mediated autophagy
CRISPR	Clustered regularly interspaced short palindromic repeats
COX	Cytochrome c oxidase
cryo-EM	Cryogenic electron microscopy
CTE	Chronic traumatic encephalopathy
CYC	Mitochondrial apocytochrome c
DHM	Dihydromyricetin
DLB	Dementia with Lewy bodies
DSS	Disuccinimidyl suberate
FC	Flow cytometry
FFI	Fatal familial insomnia
FITC	Fluorescein isothiocyanate
FITC-dextran	Fluorescein isothiocyanate–Carboxymethyl–Dextran
FRET	Fluorescence resonance energy transfer
FTD	Frontotemporal dementia
GCI	Glial cytoplasmic inclusions
GWAS	Genome-wide association study
HTS	High-throughput screening
iN	Induced neurons
iPSC	Induced pluripotent stem cells
IDP	Intrinsically disordered protein
KEGG	Kyoto Encyclopaedia of Genes and Genomes
KO	Knock out
LB	Lewy bodies
LDH	Lactate dehydrogenase
L-DOPA	Levodopa
LFC	Log2 fold change
LN	Lewy neurites
MAGeCK	Model-based Analysis of Genome-wide CRISPR-Cas9 knockout
MAP	Microtubule-associated protein
MAPS	Misfolding associated protein secretion
MPTP	1-methyl-4-phenyl-1,2,3,6-tetrahydropyridine
MS	Mass spectrometry
MSA	Multiple system atrophy
MSD	Mean square displacement

NAC	Non-amyloid β component
NDDs	Neurodegenerative diseases
NDUF	NADH:ubiquinone oxidoreductase
NMDAR	N-methyl-D-aspartate receptor
OMIM	Online Mendelian Inheritance in Man
OPCA	Olivopontocerebellar atrophy
p38 MAPK	p38 Mitogen Activated Protein Kinase
PARK2	Parkin / RBR E3 Ubiquitin Protein Ligase
PCA	Principal component analysis
PCC	Pearson's correlation coefficient
PD	Parkinson's disease
PFFs	Pre-formed fibrils
PKC	Protein kinase C
PrPC	Cellular prion protein
PrPSc	Scrapie isoform of the prion protein
p-α-Syn	Phosphorylated α-synuclein
RBD	Rapid eye movement sleep behavior disorder
REM	Rapid eye movement
SalB	Salvianolic acid B
SDS	Shy-Drager Syndrome
sgRNA	Single-guide RNA
SMT	Single molecule tracking
SND	Striatonigral degeneration
SNpc	Substantia Nigra pars compacta
Synph-1	Synphilin-1
SPE	Single primer extnesion
TFEB	Transcription Factor EB
UMIs	Unique molecular identifiers
WT	Wild type
XRD	x-ray diffraction
YFP	Yellow fluorescent protein
α-Syn	α-Synuclein

Introduction

Synucleinopathies

Synucleinopathies are a subset of neurodegenerative diseases characterised by a shared hallmark, the misfolding of the neuronal presynaptic protein α-synuclein (α-syn). Among these diseases are Parkinson's disease (PD), Dementia with Lewy bodies (DLB) and Multiple system atrophy (MSA) (Atsushi *et al.* 2006).

These three diseases are late-onset neurodegenerative disorders, with distinct manifestations depending on the affected brain region and cell type (Wenning *et al.* 1994; Martí *et al.* 2003; Stoker and Greenland 2018; Arnaoutoglou *et al.* 2019). While the role of misfolded α-syn in disease aetiology remains mostly unknown, the relevance is clear from the co-occurrence of α-syn aggregation in the regions impacted by pathology (Figure 1).

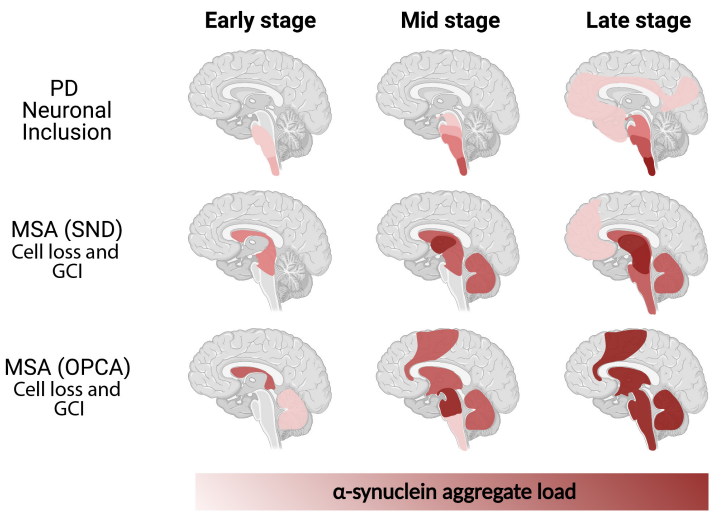

Figure 1 | Overview of neuropathological progression for synucleinopathies. Synucleinopathies display their own aetiology and as a consequence have their own progression of neuropathology. Aggregation of α-synuclein occurs in three distinct type of inclusions in three clinical syndromes: Parkinson's disease (PD), Dementia with Lewy bodies (DLB), and Multiple system atrophy (MSA). MSA is commonly divided into different clinical phenotypes due to the distinct localization of the lesions: olivopontocerebellar atrophy (OPCA) and striatonigral degeneration (SND). Here the progression from early, to mid and late stage disease is depicted, with an increase severity of α-synuclein pathology in the indicated neuronal region given by an increase in the intensity of color. GCI: Glial cytoplasmic inclusions. Adapted from (Marui *et al.* 2002; Braak *et al.* 2004; Halliday 2015)

Parkinson's disease

The first clear medical description of PD was given in the 1817 monograph "An Essay on the Shaking Palsy" by James Parkinson (Parkinson 1817). The essay focused on six individuals diagnosed with what was termed "paralysis agitans", presenting with tremor, slowed movements, and gait impairment. It was not until 1880 that the disease manifestation was refined by Jean-Martin Charcot and later became referred to as "Parkinson's disease" (Shulman *et al.* 2011; Walusinski 2018).

The defining neuropathological hallmarks of PD, the Lewy bodies (LB) and Lewy neurites (LN), were described in 1912 by Friedrich Lewy after whom they were named (Lewy 1912). He described these frequently co-exisiting inclusions as "amylaceous bodies or corpuscles", and were further defined by their characteristic bright red staining with Mann's technique (methyl blue-eosin mixture) (Engelhardt and Gomes 2017). Fifty years later, in the 1960s, examinations by phase and electron microscopy revealed the content of the inclusions to be rich in filament structures, which would in 1997 be identified as fibrillar α-syn (Duffy and Tennyson 1965; Spillantini *et al.* 1997).

In the pathological setting, LB and LN are observed in dopaminergic neurons initially in the brainstem and later with the onset of motor symptoms in the midbrain (Braak *et al.* 2003). Motor symptoms manifest as dopaminergic neurons are lost or become dysfunctional leading to a deficiency in dopaminergic signalling. Overcoming this deficit is the base for the mainstay symptomatic treatment of PD motor symptoms, dopamine replacement therapy. This is most commonly done by prescribing levodopa (L-DOPA), which is converted to dopamine in the striatum (Lloyd *et al.* 1975).

Uncertainty remains regarding the involvement of LB and LN as either cause or consequence of the ongoing pathology (Chartier and Duyckaerts 2018). The dichotomy stems from a hypothesis stating LB and LN are aggresome-related structures meant to sequester detrimental aggregated α-syn species, instead of being toxic themselves (Olanow *et al.* 2004). This topic of α-syn-induced toxicity will be

discussed in further detail later.

The involvement of α-syn in the pathology of PD was further emphasized by the discovery of the A53T missense point mutation in a family from Contursi in Italy that led to an autosomal dominant form of PD (Golbe *et al.* 1996). Since then, 18 genes have been found to lead to inheritable forms of PD and are recognized by their designation as PARK genes. Among the proteins encoded by these genes are α-syn (*SNCA, PARK1,4*), parkin (*PARK2*), LRRK2 (*LRRK2, PARK8*) and VPS35 (*VPS35, PARK17*). A recently updated list of monogenic PD-loci described in the Online Mendelian Inheritance in Man (OMIM) is shown in table 1 (Stoker and Greenland 2018). Such familial monogenetic forms of PD are assumed to account for 3-5% of overall PD cases, while the remaining is thought to arise from a mix of polygenic risk scores and environmental factors (Nalls *et al.* 2019).

Location	Gene	PARK	Inheritance	OMIM number
4q22.1	SNCA	PARK1/PARK4	Autosomal dominant	163890
4p13	UCHL1	PARK5	Autosomal dominant	191342
1p36.12	PINK1	PARK6	Autosomal recessive	608309
1p36.23	DJ1	PARK7	Autosomal recessive	602533
12q12	LRRK2	PARK8	Autosomal dominant	609007
1p36.13	ATP13A2	PARK9	Autosomal recessive	606693
2q37.1	GIGYF2	PARK11	Autosomal dominant	607688
2p13.1	HTRA2	PARK13	Autosomal dominant	610297
22q13.1	PLA2G6	PARK14	Autosomal recessive	603604
22q12.3	FBXO7	PARK15	Autosomal recessive	605648
16q11.2	VPS35	PARK17	Autosomal dominant	601501
3q27.1	EIF4G1	PARK18	Autosomal dominant	600495
1p31.3	DNAJC6	PARK19a	Autosomal recessive	608375
21q22.11	SYNJ1	PARK20	Autosomal recessive	604297
3q22		PARK21	Autosomal dominant	616361
4q22.1	VPS13C	PARK23	Autosomal recessive	608879

Table 1 | Overview of known familial monogenic variants. Genes in which a mutation leads to monogenic familial PD are listed along with their inheritance pattern and OMIM number for reference. Both gene name and PARK number is displayed where available.

Clinically, the progression of PD is described as having a prodromal and a symptomatic phase. The prodromal phase can occur 12-14 years prior to onset of motor symptoms, and include symptoms such as loss of smell, constipation and rapid eye movement (REM) sleep behaviour disorder (RBD) (Postuma *et al.* 2012). During this phase, neuropathological changes are observed in the medulla oblongata and olfactory bulb (Braak *et al.* 2003). With later neurodegeneration in the midbrain, motor symptoms manifest. At later stages, cognitive symptoms appear as the higher brain areas are also affected by the pathology and degeneration (Braak *et al.* 2003) (Figure 1).

A unified staging hypothesis was proposed based on the post-mortem characterization of LB pathology by Braak and colleagues, referred to as Braak's hypothesis (Braak *et al.* 2003). This proposed staging paradigm correlates severity of LB pathology in brain regions with disease progression divided into 6 stages. The first three are pre-symptomatic and the last three are symptomatic. The progression of the stages depicts a spreading pattern of LB pathology along anatomically interconnected areas in the brain (Figure 1).

Dementia with Lewy bodies

Dementia is a common age-related diagnosis with 10 million new diagnoses worldwide per year. Among dementias, DLB account for ~4-7% of clinically diagnosed dementias in western populations (Arnaoutoglou *et al.* 2019). This prevalence may be underreported as DLB has frequently been misdiagnosed as other types of dementia such as Alzheimer's disease (AD) (Litvan *et al.* 1998).

The first report on DLB originated in 1984, where the disorder was described as "diffuse Lewy body disease" by Kenji Kosaka's post-mortem study of a presenile dementia case (Kosaka *et al.* 1984). Unlike PD, with which DLB shares the hallmark of LBs, the pathology in DLB seems to originate as cortical pathology and later spread towards more central brain areas (Marui *et al.* 2002).

The distinct progression of DLB compared to PD is clear from the diagnostic criteria for DLB, which emphasizes a cognitive decline, memory impairment and deficits in attention and executive function among others. In addition to cognitive impairments, as the disease progresses, parkinsonian motor symptoms may also occur (McKeith *et al.* 2017).

Multiple system atrophy

Similar to PD and DLB, MSA is a chronic, progressive neurodegenerative disorder, but unlike the other synucleinopathies, MSA is ultimately fatal. The median survival ranges from 8.5-9.5 years after onset of first symptoms (Wenning *et al.* 1994; Schrag *et al.* 1999). Compared to PD and DLB, MSA occurs more rarely with an estimated prevalence of 4.4:100.000 persons per year (Schrag *et al.* 1999).

The first documented clinical cases of MSA date back to 1900, where it was termed olivopontocerebellar atrophy (OPCA) based on the brain regions affected (Marmion *et al.* 2021). Later descriptions of what we today classify as subtypes of MSA were described as Shy-Drager syndrome (SDS) and striatonigral degeneration (SND), also dependent on the distinct affected regions in the brain (Figure 1). The major subtypes among these three are OPCA which presents with cerebellar ataxia and SND, clinically presenting as a parkinsonian syndrome, and possibly with autonomic failure (Brettschneider *et al.* 2018). Due to the symptomatic overlap of SND and PD, prior to the advent of L-DOPA treatment for motor symptoms for PD, misclassification would frequently occur (Marmion *et al.* 2021). A defining characteristic for SND is the non-/poor responsiveness to L-DOPA treatment, which was later identified and has become a feature for clinical assessment of patients. (Wenning *et al.* 1994)

A main point of contrast between MSA and PD or DLB is the neuropathological hallmarks. While neuronal inclusions are found in MSA, the main hallmark is instead depositions in oligodendrocytes, where the aggregates are temred glial cytoplasmic inclusions (GCIs) (Marmion *et al.* 2021).

Biology of α-synuclein

α-syn is a highly conserved neuronal protein composed of 140 amino acids encoded by the *SNCA* gene. It was initially reported to be an intrinsically disordered protein (IDP), signifying a lack of secondary structure. However, recent experimental findings have suggested the native state may instead be tetrameric, a topic that will be addressed later. It belongs to the synuclein family of proteins which is comprised of three members; α-, β- and γ-synuclein, of which α-syn is the only disease-related protein (George 2001). The primary sequence of α-syn can be divided into three domains based on their structural and biochemical properties.

The N-terminal (residues 1-60) contains 6 imperfect KTKEGV repeat motifs and facilitates binding to negatively charged membranes. Upon this binding, monomeric α-syn can adopt an alpha-helical secondary structure. The second domain is the non-amyloid β component (NAC) (residues 61-95). This domain was initially discovered as a peptide associated with senile plaques in AD, which is where it derived its name from (Dickson 1999). The NAC domain has been found to form the core of the fibrillar α-syn, where it adopts a "Greek key" motif with the characteristic amyloid cross-β-sheet structure. Lastly, the C-terminal (residues 96-140) is highly charged, and is involved in metal iron- and protein-binding, among other functions (Figure 2).

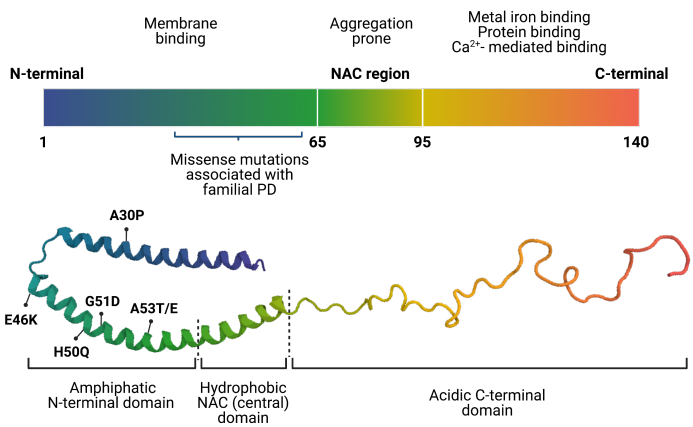

Figure 2 | Structural characterization of α-synuclein. α-synuclein is composed of 140 residues which can be divided based on regional properties. Here a depiction of the three main domains: the lipid binding N-terminal, the central non-amyloid β component (NAC) region, and the acidic C-terminal, along with the corresponding secondary structure. The locations of chracterised missense mutations leading to familial PD are noted within the N terminal domain.

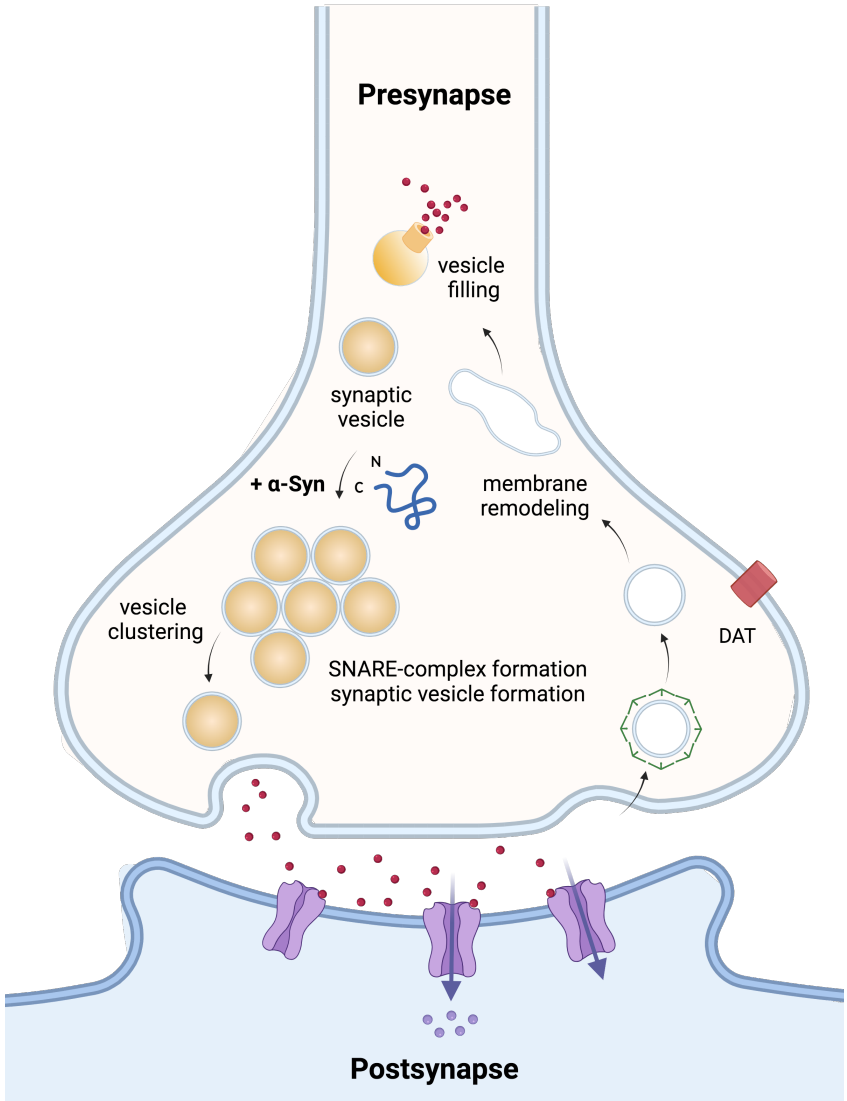

Figure 3 | Physiological functions of α-synuclein at the synapse. The physiological role of α-synuclein is not well understood, but its involvement in neuronal function at the synapse has been demonstrated. Shown are the main functions in which α-synuclein has been reported to be involved in. These synaptic processes include membrane remodeling, modulation of the dopamine transporter (DAT), maintenance of the synaptic vesicle pool, clustering and recruitment of vesicles to the plasma membrane, and priming for release by promoting SNARE-complex assembly. Adapted from (Burré 2015)

In the cellular context, α-syn is primarily observed to be a neuronal protein, found both at the pre-synapse and in the nucleus. Currently, understanding of the physiological function of α-syn is still poorly understood for both synaptic and nuclear locations; however, we have a slightly better understanding of the function at the synapse (Figure 3). At the synapse, α-syn has been observed to assist in maintaining the synaptic vesicle pool by tethering synaptic vesicles together. Interactions with SNARE proteins have also been described, a superfamily of proteins that drive membrane fusion and exocytosis of neurotransmitters, suggestive of a potential role of α-syn in synaptic vesicle release (Figure 3) (Burré 2015).

The potential role in maintaining synaptic function is further underlined by observations in αβγ-synuclein knockout mice, a mouse models which lack all proteins in the synuclein family. While deletion of synucleins was not lethal, it caused alterations in synaptic structure and firing, shedding evidence of the involvement of synuclein in neuronal function (Greten-Harrison *et al.* 2010).

α-synuclein pathology

The process of pathological misfolding of α-syn into amyloid fibrils is dependent on the adoption of a cross-β-sheet structure which is characteristic of all amyloid fibrils (Jahn *et al.* 2010). The process of conversion from the native intrinsically disordered state into fibrillar α-syn has been shown to be a nucleation-dependent process (Wood *et al.* 1999). This entails that monomeric α-syn exists in an equilibrium with the oligomeric form that can serve as a seed for fibril formation. This initial seed formation is the rate-limiting step in fibril formation, and an exponential growth of α-syn fibrils is seen following the initial seed formation (Figure 4).

The process of α-syn fibril formation at physiological conditions, that is, at 37 °C and neutral pH, is a reluctant process and will seldom occur in absence of agitation or a surface such as a liquid-air interface to facilitate nucleation (Campioni *et al.* 2014, 2020; Zhou *et al.* 2020). However, by altering reaction conditions and accelerating the formation of the initial nucleus, aggregation formation can be accelerated. Such changes include increasing the α-syn monomer concentration, lowering the pH, increasing salt concentration, crowding the molecular environment and applying agitation. Changing these parameters during fibril assembly has an impact on the likelihood of the formation of the initial seed. Shortening the duration of the rate-limiting step thereby also accelerates the overall process of fibril formation.

The effect of changes in physiological conditions on α-syn fibril assembly have also been partially observed from patient pathology and cell-based studies. From patient genetic analysis, duplication/triplication mutations in the *SNCA* gene were shown

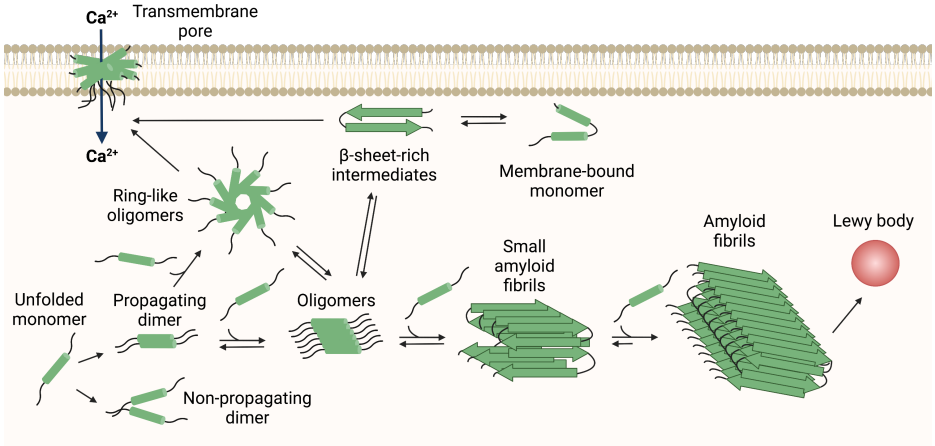

Figure 4 | Diagram of the aggregation process of α-synuclein. The aggregation of α-synuclein is a nucleation-dependent process, where the rate-limiting step is formation of the initial seed. Along the process, α-synuclein is in equilibrium mostly favouring the monomeric state. Once the initial seed is formed, the thermodynamic stability of the amyloid fibril favours elongation of fibrils and thereby recruits α-synuclein to the fibril structure in a stepwise manner, formic larger multimeric protein species. During the fibrillation process, α-synuclein can be found as a monomer, an oligomer of various structures or associated with membranes. Such species, as well as PFFs, may also drive pathology by acting as seeds for the formation of additional aggregates. Adapted from (Lashuel *et al.* 2013)

to be linked with familial PD, establishing a direct link between α-syn concentration and disease onset. Similarly, the *SNCA* gene has also been described to harbour other missense familial mutations such as A30P and A53T (Figure 2), shown to decrease the native membrane binding capacity. This altered affinity for membranes increases the free α-syn monomer concentration and is believed to be part of the underlying pathophysiological mechanism for the development of familial PD.

True prions

Prions are pathogenic particles composed of misfolded proteins, capable of transferring from cell-to-cell and initiating templated seeding. Templated seeding promotes natively folded proteins to adopt the prion structure, whereby successive rounds of transmission and seeding can drive the pathology (Figure 5). Prion diseases are associated with the cellular prion protein (PrPC), from which the name is derived, which upon conformational conversion, turns into its misfolded pathogenic form (PrPSc). Interestingly, as the aggregated PrPSc acts as a pathogenic particle, it can lead to different diseases depending on the conformation of the aggregated PrPSc protein. This can be seen in humans from the large diversity in prion diseases such

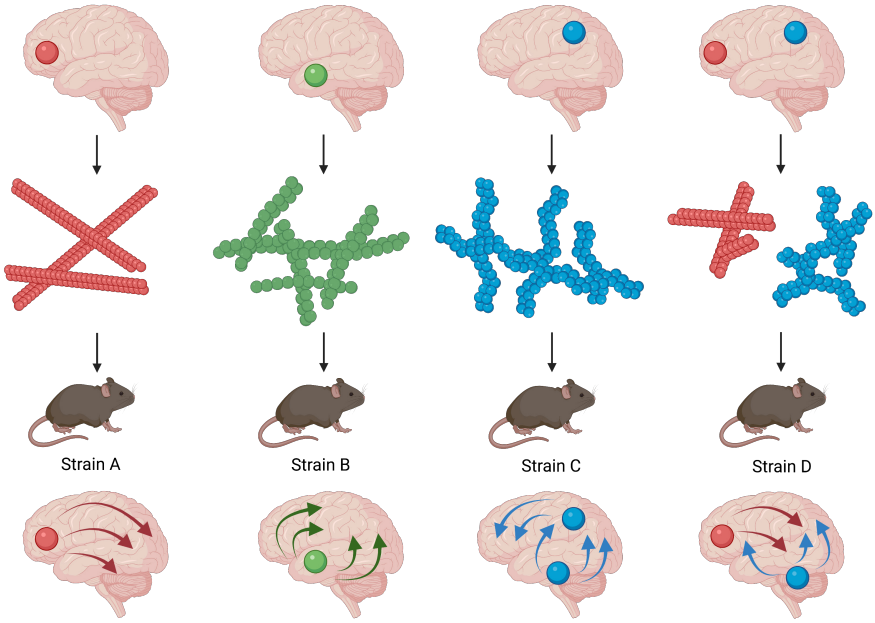

Figure 5 | The prion model for progression and heterogeneity of neurodegenerative diseases. Prion diseases are the first examples where the pathogen is a protein capable of transmitting and replicating on its own. As the pathogenic nature is derived from its conformation, variations in structure can also lead to distinct pathologies with unique aetiology and symptoms. Prion diseases are furthermore capable of propagating and replicating the conformation faithfully. Therefore, a purified seed of strain A can be injected into a new recipient and will lead to identical pathology. Similarly, if multiple prions are injected simultaneously, both pathologies will be induced in the recipient based on the injected strains. Adapted from (Stopschinski and Diamond 2017)

as Creutzfeldt-Jacobs disease (CJD), Kuru and Fatal familial insomnia (FFI) . Among the animal prion diseases exists Scrapie, Transmissible mink encephalopathy (TME) and bovine spongiform encephalopathy (BSE) (Ma and Wang 2014).

A prion-like hypothesis

One of the earliest suggestions of a prion-like spread for synucleinopathies was in PD pathology, in the initial publication of Braak's hypothesis (Braak *et al.* 2003). Based on the orderly spread through anatomically interconnected areas, it was hypothesized that a neurotropic pathogen may be the cause of disease. Evidence for such a transfer of α-syn pathology was later reported from two independent follow-up studies on cell replacement trials for PD. Both reports found LB pathology in engrafted fetal dopaminergic neurons only 11-16 years after successful engraftment (Kordower *et al.* 2008; Li *et al.* 2008). As this is far younger than expected for cells

to develop LB pathology on their own, it was suggested that a host-to-graft spread was the cause.

Such cell-to-cell spread of α-syn pathology has since been observed in cell-based studies both *in vitro* (Reyes *et al.* 2015) and *in vivo* (Angot *et al.* 2012). A notable demonstration of prion-like transmissibility is the intercranial injection of α-syn PFFs leading to α-syn pathology in non-transgenic mice (Luk *et al.* 2012). Similar experiments have been carried out showing the possibility of induced pathology transferring to the brain from either the olfactory bulb (Rey *et al.* 2013, 2018) or enteric neurons (Holmqvist *et al.* 2014). Such a spread from periphery towards the brain is possible in animal models gives further credence to Braak's hypothesis, as well as giving value to the potential gut-to-brain or nose-to-brain axis of pathology.

A prion-like spread has also been demonstrated using brain lysates from MSA patients. When injected or administered, the patient brain lysate was able to propagate aggregation in both cell and animal models of synucleinopathy. Furthermore, strain-like properties were maintained through subsequent serial passaging of the brain lysate in mice (Prusiner *et al.* 2015; Woerman *et al.* 2019). Interestingly, patient brain lysate from PD showed negligible ability to induce α-syn aggregation despite the presence of LB pathology (Prusiner *et al.* 2015). This indication of differential capacity to seed α-syn aggregation could explain the more rapid disease progression seen in MSA compared to patients with PD. It also raises the question of whether α-syn aggregates can be conformationally different leading to potential distinct α-syn strains.

Structural and Functional Insights into α-Synuclein Fibril Polymorphism

As mentioned above, there may be conformational differences between α-syn aggregates purified from MSA compared to PD patient brains. Similar results have been shown in a comparison study between GCI-derived α-syn and LB-derived α-syn, where conformational and biological differences were observed (Peng *et al.* 2018). It was also observed that the intracellular milieu could influence the conformation of aggregate formed within the recipient cell (Peng *et al.* 2018).

A different approach to generating conformationally distinct α-syn is by modulating the conditions for fibril assembly using recombinant protein. This was among the first demonstrations that conformationally distinct α-syn fibrils could be generated based on the application of various biophysical methods, including x-ray diffraction (XRD) and limited proteinase K digestion (Bousset *et al.* 2013). These reported conformationally distinct α-syn PFFs were also shown to have differential effects *in vivo* after injection into rat brain, resulting in distinct α-syn pathologies (Peelaerts *et al.* 2015).

Within other proteinopathies, similar strain hypotheses have been suggested. One

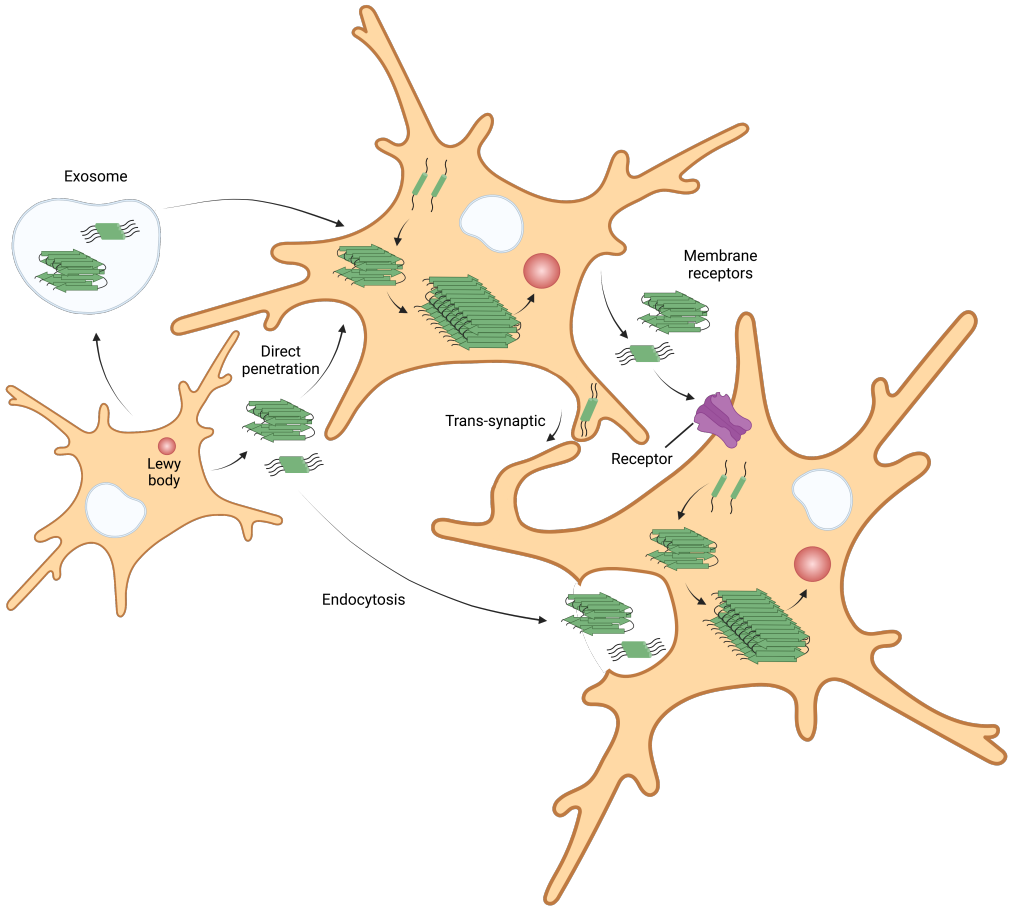

Figure 6 | Overview of mechanisms potentially underlying prion-like spread of α-synuclein. The hypothesis of a prion-like spread is depicted here, commencing with an initial cell in which the α-synuclein aggregation originates. Spread from the host cell to potential recipients can occur through numerous different routes. Exosomal release of vesicular enclosed α-synuclein can transfer aggregate directly between cells. Direct secretion of seed material can deposit seeds in the extracellular space for recipient cells to internalize through endocytosis, phagocytosis, or direct penetration. Trans-synaptic or receptor-mediated spread has also been highlighted as a method of propagation of α-synuclein aggregates. In common for all methods of spread is the expectation that the seed material gains cytosolic entry whereby it can induce aggregation of the recipient cells with natively folded α-synuclein. Adapted from (Lashuel *et al.* 2002)

of the best documented cases is the microtubule-associated protein (MAP) tau, which is involved in a range of neurodegenerative diseases. Recently, a series of cryogenic electron microscopy (cryo-EM) studies have examined the structure of tau fibrils and found distinct conformations for each associated disease. These tau fibrillar structures have been reported for AD (Fitzpatrick *et al.* 2017; Falcon *et al.* 2018b), frontotemporal dementia (FTD), Pick's disease (Falcon *et al.* 2018a), chronic traumatic encephalopathy (CTE) (Falcon *et al.* 2019) and corticobasal degeneration (CBD) (Zhang *et al.* 2020).

If strains prove to be a fundamental phenomenon within synucleinopathies, that could help explain the varied pathology that differentiates PD, DLB, MSA and other synucleinopathies.

Prion-like cell-to-cell transmission

At present, our understanding of the molecular events that may be involved in a prion-like spread has remained elusive. Recent findings have suggested pathways that may be involved in a prion-like spread, but multiple routes have been suggested and may depend on the investigated model system. In general, for a prion-like spread to occur in the way that was described by Braak and colleagues, a spread of α-syn pathology should occur through anatomically interconnected regions. For this spread to happen, four key events should occur. First, an initial aggregation event initiates. Secondly, the misfolded material should leave the cell. Third, a recipient cell must internalize the secreted seeding material, and last, it must enter the cytosol where it can initiate the aggregation cycle again (Figure 6) (Lashuel *et al.* 2002).

Modes of action to facilitate each of these steps have been reported with multiple possibilities for each step. For cell secretion of potential misfolded α-syn, exosomes are thoroughly been studied as vehicles (Alvarez-Erviti *et al.* 2011; Danzer *et al.* 2012; Si *et al.* 2019; Guo *et al.* 2020). Novel pathways such as misfolding associated protein secretion (MAPS) have also been reported (Lee *et al.* 2016). While the exosomes themselves facilitate the transfer to recipient cells, non-vesicular enclosed α-syn aggregates have to be internalized by recipient cells. Recent studies have shown that membrane receptors such as LAG3 and APLP1 may interact with misfolded α-syn to facilitate this uptake, although this putative hypothesis is still a debated topic (Mao *et al.* 2016). Following cellular uptake by endocytic processes, α-syn aggregates have been shown to escape the endo-lysosomal enclosure by permeabilizing membranes, gaining access to the endogenous pool of α-syn and inducing aggregation. Lastly, other methods for transfer have also been reported such as trans-synaptic spread and tunnelling nanotubes (Figure 6).

α-*synuclein as a tetramer*

An alternative hypothesis to the classical picture of α-syn aggregation from monomer to fibril is the tetramer hypothesis postulated by Dennis Selkoe and colleagues (Bartels *et al.* 2011; Dettmer *et al.* 2015b, a). They have described a novel state of physiological α-syn, namely as a tetrameric structure. This structure has previously been reported as the native conformation of α-syn, but due to detergent containing buffers used for routine cell extraction, the tetramer is denatured to α-syn monomers (Bartels *et al.* 2011). By running native-PAGE or performing crosslinking with disuccinimidyl suberate (DSS), α-syn tetramers were readily identifiable on western blotting in HEK293, HeLa, M17D, COS-7, human red blood cells and mouse cortex (Bartels *et al.* 2011). Importantly, these tetramers formed stable structures in cellular contexts that underwent little aggregation. The formation of tetrameric structures was attributed to the KTKEGV domain within the N-terminal region, and disruption of these domains was found to lead to apparent neurotoxicity (Dettmer *et al.* 2015a). Likely mechanisms for this phenomenon are the disruption and disassembly of α-syn tetrameric structures, and a concomitant increase in monomeric α-syn, increasing the free α-syn concentration that can undergo aggregation (Dettmer *et al.* 2015b).

The most elegant demonstration of the existance of α-syn tetramers and the importance of tetramer disruption is the generation of a mouse model based on tetramer disruption. This mouse model expresses the E46K mutation in α-syn associated with familial PD, with an additional 2 homologous E to K mutations in the adjacent KTKEGV domains. This resulted in a mouse model that recaptures many important aspects of PD; loss of nigrostriatal dopaminergic neurons, post-translationally modified α-syn aggregation, motor deficits, and responsiveness to levodopa (L-DOPA), a precursor to dopamine. (Nuber *et al.* 2018)

Even with the impressive supportive data, the topic of a potential tetrameric structure adopted by α-syn is still debated as some research groups report issues with replicating the findings (Alderson and Bax 2016). However, in recent years, more reports documenting the α-syn tetrameric conformation are coming forth with interesting implications (Fernández and Lucas 2018; Kim *et al.* 2018; Glajch *et al.* 2021).

The study of α-synuclein aggregation

In an attempt to better understand the complex intricacies of biological phenomena, experimental systems have been leveraged to recreate aspects of human disease and build a foundational knowledge. Within the field of study of synucleinopathies, disease modeling is helping elucidate the molecular basis underlying pathogenesis

and characterise the mechanisms whereby PD pathology becomes widespread. Over the last decades, the landscape of experimental models has been changing exponentially. There has been a shift from uniquely relying on post-mortem neuropathological examinations of patients, to more sophisticated *in vitro* and *in vivo* cell-based and murine models.

Early investigations into the broader nature of progression of disease pathology in the brains of PD patients have given us an understanding of which regions of the brain and cell types are especially vulnerable to disease (Figure 7). This has in turn lead to the establishment of toxin-based animal models that mimic the cell loss observed in patients. Models using toxins such as 6-hydroxydopamine (6-OHDA) and 1-methyl-4-phenyl-1,2,3,6-tetrahydropyridine (MPTP) (Simola *et al.* 2007). These models have long been used to investigate PD-related motor dysfunction as they can cause a substantial loss of dopaminergic neurons leading to dysfunction in dopamine signalling (Blum *et al.* 2001; Schober 2004). While these toxin models of PD elicit behavioural abnormalities such as rotational asymmetry in rats upon unilateral lesion, the models come with their own shortcomings. For instance, cell loss is required from the toxin-based lesion, where it has been reported that more than 80% of dopaminergic neuron loss is needed for behavioural changes to occur (Chang *et al.* 1999). Other departures from PD include modeling a chronic progressive disease in an acute toxin-based model, the lesions are almost exclusively dopaminergic, and animals lack the characteristic LB inclusions.

Refinement of model systems, and subsequent development of our current model systems comes in part from the understanding of synucleinopathies at the genetic level. Genome-wide association studies (GWAS) in PD patients have identified both monogenetic variants for PD but also a number of polygenic risk scores. An early example of this translation of genetic information to model systems is seen with Saccharomyces cerevisiae, also known as baker's yeast. While among the simplest of cellular models, it also allows for rapid experimentation. This advantage has been leveraged to discover several milestones in synucleinopathies, such as the relevance of heat shock proteins in preventing α-syn toxicity (Flower *et al.* 2005) as well as the importance of phosphorylation in clearance of α-syn aggregates (Tenreiro *et al.* 2014). Other interesting findings have emerged from early disease modeling in yeast, such as the characterization of α-syn aggregates (Zabrocki *et al.* 2005), compound screening for modulators of aggregation (Griffioen *et al.* 2006) and genome-wide screens to identify enhancers of α-syn toxicity (Willingham *et al.* 2003).

Improved understanding of the underlying genetics has also led to an abundance of more complex model systems. These experimental systems range from yeast, immortalized cell lines, primary neurons, differentiated immortalized cell lines and ultimately patient-derived stem cells such as induced pluripotent stem cells

(iPSCs) and induced neurons (iNs). Of equal complexity to iPSCs and iNs are genetic animal models, which provide an invaluable tool for the study of complex interactions between all resident cell types in the brain (Figure 7). Within the PD animal models available, the 3K mouse model developed by Denis Selkoe stands out as a good example of a model where physiological and behavioural features reminiscent of human PD have been successfully reproduced. (Nuber *et al.* 2018) (Delenclos *et al.* 2019).

The work presented in this thesis tries to find a balance in terms of complexity and output. Using immortalized cell lines, we are able to scale the scope of our studies all the way to genome-wide studies, while still working in human-derived cell lines. Moving closer to human disease with currently available methods becomes costly due to reagent cost of generating iPSCs or iNs at scale, and currently performing such screens in animal models is unfeasible. These considerations in terms of which model is best suited to address the specific goals of the experimental approach is therefore of great importance.

Through the work presented here, we progressively refine our model systems and attempt more complex experimental modalities as we refine them.

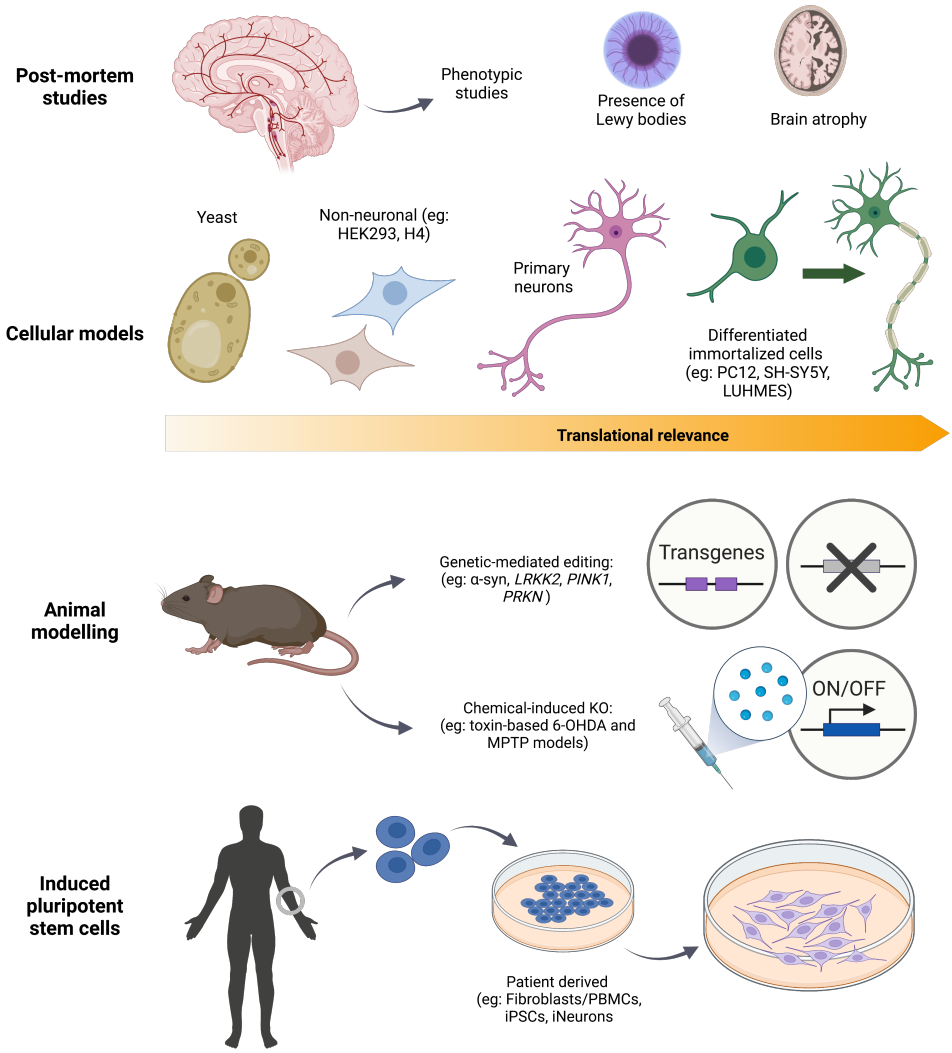

Figure 7 | Overview of various approaches to investigate and model α-synuclein aggregation. Our understanding of synucleinopathies comes initially from the study of the disease where it occurs. For neurodegenerative diseases this is frequently post-mortem or other clinical studies. In terms of model systems there is a gradient of complexity from simple cell-based models towards more intricate systems such as animals or stem cell-based models. An inverse correlation between model complexity and throughput exists but is balanced by the increased relevance to the disease in question. Adapted from (Delenclos *et al.* 2019; Avazzadeh *et al.* 2021)

Aims of the thesis

The focus of this thesis has been to identify and characterise cell-intrinsic mechanisms driving α-syn aggregation and understand the molecular mechanisms that play a part in α-syn-related pathology. These studies resulted in four distinct projects, each addressing the following objectives we sought to achieve:

I Examine the impact of pathologically relevant α-syn (mutant and fibrillar) on mouse primary hippocampal neurons. Specifically, characterize the effects exerted on NMDAR membrane dynamics. (Paper I)

II Establish a model for α-syn aggregation and investigate compounds with known neuroprotective effects. Identify mode of action involved in regulation of α-syn pathology. (Paper II)

III Having shown the potential for mechanistic investigation of α-syn aggregation in cell lines, establish a model system scalable for high-throughput screening. Show efficacy of screening-based approaches for identification of modulators of α-syn aggregation. (Paper III)

IV Perform genome-wide screening as an unbiased approach to elucidate gene function, identify novel genetic modulators of α-syn aggregation and characterise the gene networks involved. (Paper IV)

Summary of key results

Paper I

Impact of pathological α-synuclein on mouse neurons

In order to characterise the cause-and-effect relationship between α-syn aggregation and neurodegeneration, α-Syn preformed fibrils (PFFs) have been used to inoculate primary neurons *in vitro* and *in vivo*. These models have recapitulated most features exhibited during pathologic α-Syn aggregation, including phosphorylated α-syn (p-α-Syn) positive inclusions, neuronal loss, activated inflammatory response and impaired dopamine release (Kirik *et al.* 2002; Volpicelli-Daley *et al.* 2011; Paumier *et al.* 2015; Harms *et al.* 2021). Among the findings resulting from these studies, α-Syn overexpression and α-Syn PFFs were shown to decrease expression of synaptic proteins, cause neurotoxicity and consequently lead to neuronal cell death (Volpicelli-Daley *et al.* 2011). One such protein, found to be affected by the aggregation of α-syn is the N-methyl-D-aspartate receptor (NMDAR). Experimental evidence have shown α-syn-induced alterations in NMDAR expression, long term potentiation and subcellular localization (Emanuele *et al.* 2016; Tozzi *et al.* 2016; Ferreira *et al.* 2017; Durante *et al.* 2019). Despite the increasing amount of data linking NMDAR with α-syn-based pathology, the mechanisms by which pathological α-syn effects membrane dynamics of NMDARs is still lacking.

With the aim of elucidating the impact of α-syn on neuronal NMDAR membrane dynamics, we apply quantum dot labelling of NMDAR subunits, Glu2A/Glu2B, to perform single molecule tracking (SMT) analysis at the neuronal post-synapse. This investigation was performed for both transfection-mediated α-syn overexpression and direct addition of α-syn PFFs.

To establish a baseline for the effects of α-syn overexpression, we first investigated the NMDAR lateral diffusion in hippocampal primary neurons overexpressing

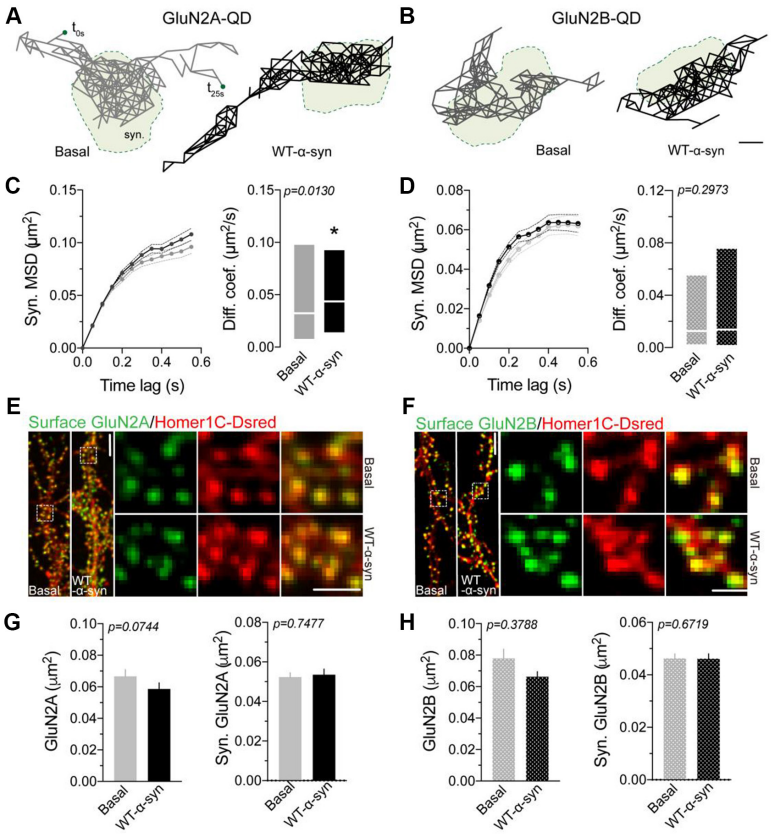

Figure 8 | Effect of α-synuclein overexpression on NMDAR diffusion and expression. **A-B)** Representative trajectories from single particle tracking experiments (~25 s duration) from GluN2A (A) and GluN2B (B) (scale=200nm). **C)** Left: Mean square displacement (MSD) of synaptic GluN2A-QD over time of basal (grey) and WT-α-synuclein (black). Right: Diffusion coefficients for basal and WT-α-synuclein overexpression. (n_{Bassal}=705, $n_{WT\text{-}\alpha\text{-}synuclein}$=798, p-val=0.013, Man Whitney test). **D)** Left: MSD of synaptic GluN2B-QD over time of basal (grey) and WT-α-synuclein (black). Right: Diffusion coefficients for basal and WT-α-synuclein overexpression. (n_{Bassal}=782, $n_{WT\text{-}\alpha\text{-}synuclein}$=971, p-val=0.2973, Man Whitney test). **E-F)** Representative images of cell-based immunofluorescence assays detecting co-localisation of post-synaptic marker Homer1C (red) and either GluN2A (E) or GluN2B (F) subunits (green). **G)** Left: quantification of surface GluN2A area (n_{Basal}=80 segments, $n_{WT\text{-}\alpha\text{-}synuclein}$=84 segments, p=0.0744). Right: quantification of synaptic GluN2A area (p=0.7477). **H)** Left: quantification of surface GluN2B area (n_{Basal}=78 segments, $n_{WT\text{-}\alpha\text{-}synuclein}$=85 segments, p=0.3788). Right: quantification of synaptic GluN2B area (p=0.6719)

wild type (WT) α-syn. We observed no significant decrease in receptor diffusion compared to naïve neurons for the Glu2B subunit, and rather a significant increase was observed for Glu2A (Figure 8 A-D). In addition, we observed no difference in abundance of either receptor subunit in primary hippocampal neurons by immunostaining (Figure 8 E-H).

Missense mutations of α-syn, such as the A53T mutant, have been causally associated to familiar PD (Polymeropoulos *et al.* 1997). To model gain of function, we transiently overexpressed the PD-linked α-syn^{A53T} mutant in murine primary neurons. Next, we examined the effect of α-syn^{A53T} overexpression on NMDAR diffusion compared to WT α-syn. At similar expression levels, a significant decrease in receptor diffusion was observed for both Glu2A and Glu2B (Figure 9 A-B). In addition, a concomitant local loss of subunit density was observed at the synapse (Figure 9 C-D). Functional quantification of excitation dynamics revealed that α-SynA53T overexpression also resulted in a decrease in the frequency of calcium transient events, as measured by the calcium indicator fluorophore GcAMP6 (Figure 9 E-F).

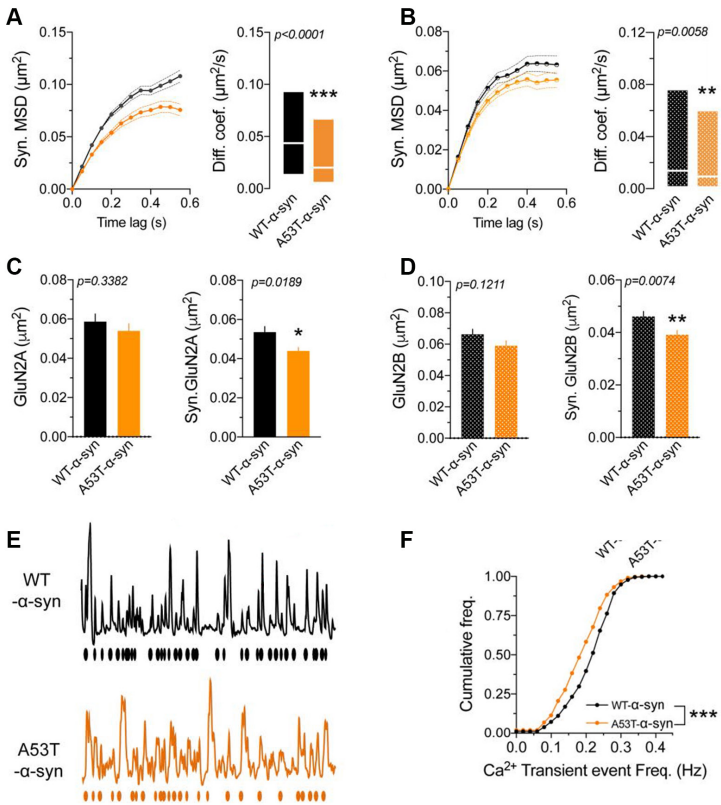

Figure 9 | Comparison of WT α-synuclein and α-synucleinA53T impact on NMDAR in neurons. A) Left: MSD of synaptic GluN2A-QD over time of WT-α-synuclein (black) and α-synuclein A53T (orange). Right: Diffusion coefficients for WT-α-synuclein and α-synuclein A53T overexpression. (n_{WT}=798, n_{A53T}=598, p-val=<0.0001, Man Whitney test). **B)** Left: MSD of synaptic GluN2B-QD over time of WT-α-synuclein (black) and α-synuclein A53T (orange). Right: Diffusion coefficients for WT-α-synuclein and α-synuclein A53T overexpression. (n_{WT}=971, n_{A53T}=844, p-val=0.0058, Man Whitney test). **C)** Left: quantification of surface GluN2A area (n_{WT}=84 segments, n_{A53T}=83 segments, p=0.3382). Right: quantification of synaptic GluN2A area (p=0.0189). **D)** Left: quantification of surface GluN2B area (n_{WT}=85 segments, n_{A53T}=79 segments, p=0.1211). Right: quantification of synaptic GluN2B area (p=0.0074). **E)** Representative traces of NMDAR mediated calcium transients (ΔF/F) F) Frequency distributions of all calcium transient events for spines in WT-α-synuclein (black) and α-synuclein A53T (orange)

Similar to the effects observed for mutant α-syn^{A53T}, a deficiency in NMDAR diffusion was observed when hippocampal primary neurons were treated with α-syn PFFs compared to monomeric α-syn (Figure 10 A). Treatment with α-syn PFFs similarly also quenched synaptic spiking activity of neurons, as seen by a decrease in the frequency of calcium transient events (Figure 10 B).

These findings contribute important insights into the aetiology and pathological impact of mutant and fibrillar α-syn on NMDA receptor organisation in neuronal systems even over shorter periods of insult.

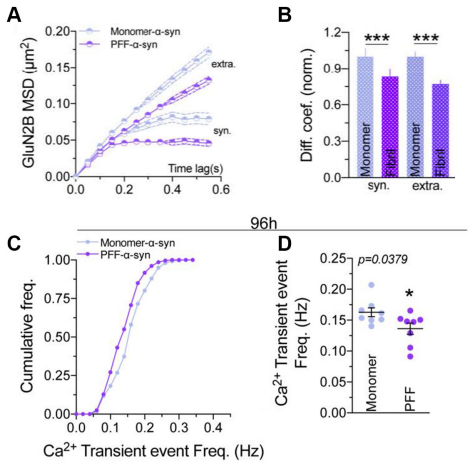

Figure 10 | α-synuclein PFF impact on NMDAR in hippocampal primary neurons. A) Mean square displacement of surface GluN2B for neurons treated with α-synuclein monomers (blue) and α-synuclein PFFs (purple). **B)** Mean diffusion coefficients for synaptic and extra-synaptic GluN2B (Synaptic: $n_{monomer}$=551 trajectories, n_{PFF}=647, p=0.0005; extra-synaptic: $n_{monomer}$ = 1048 trajectories, n_{PFF}=1250, p<0.0001, Man Whitney test). **C-D)** Calcium transients after incubation with α-syn monomers or PFFs for 96 h. (C) Frequency distribution of calcium transients and mean calcium transient frequencies ($n_{monomer}$ = 257 spines, n_{PFF} = 287 spines, ***p < 0.0001). (D) Mean calcium transient frequencies of each neuron in the respective conditions ($n_{Monomer}$ = 8 cells, n_{PFF} = 8 cells; p = 0.0379, Mann Whitney test)

Paper II

Studying α-synuclein aggregation by pharmacological interventions

To study the molecular events involved in α-syn aggregation, robust model systems that recapture the aspects in question are needed. For our initial studies, we selected the previously established synphilin-1 (synph-1) and SynT aggregation model (McLean *et al.* 2001; Bodner *et al.* 2006). This system relies on co-expression of the α-syn interacting protein, synph-1, and SynT, a C-terminal truncated α-syn-EGFP fusion protein. Immunofluorescence analysis of Syn-T transient co-transfection in H4 neuroglioma cells revealed α-syn positive aggregate formation in 50-60% of transfected cells (Figure 11 B-C). Interestingly, the Syn-T aggregation cell model trended towards an elevated cytotoxicity response, as measured by the elevated level of lactate dehydrogenase (LDH) release compared to H4 cells expressing WT α-syn. However the difference was not significant (Figure 11 D).

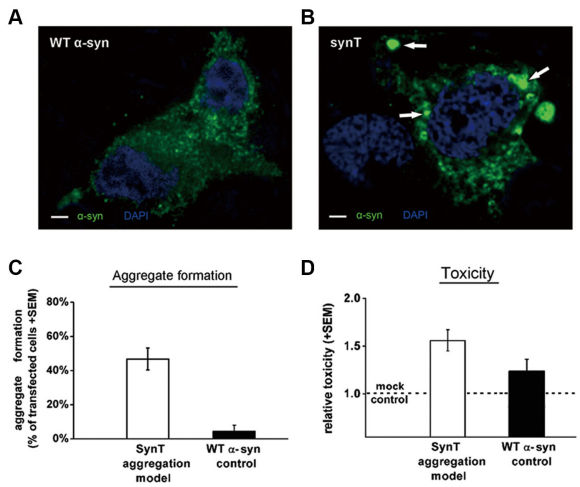

Figure 11 | Validation of Synph-1/SynT α-synuclein aggregation model in H4 neuroglioma cells. A) Overexpression of WT α-synuclein does not induce aggregate formation. **B)** Overexpression of SynT instead leads to formation of large α-synuclein aggregates (arrows). **C)** Quantification of aggregates identifies aggregates in 50–60% of transfected cells with the SynT construct **D)** Assessment of cellular viability by lactate dehydrogenase release detects no significant difference in viability between the SynT-aggregation model (n = 6) or WT α-syn control (n = 5). (Scale bar = 5 μm) (mean ± SD, *p<0.05, **p<0.01)

Using this model system, we sought to assess the effect of two small molecule compounds with known neuroprotective properties on α-syn aggregation. The compounds chosen for our study were dihydromyricetin (DHM) and salvianolic acid B (SalB) (Lee *et al.* 2013; Ren *et al.* 2016). At physiologically tolerated concentrations, a significant decrease in α-syn aggregate load was observed for both DHM and SalB (Figure 12). A concomitant increase in lysosome-associated membrane proteins LAMP1 and LAMP2A, known interactors in autophagy and chaperone-mediated autophagy (CMA), suggested a possible involvement of these degradative pathways (Eskelinen 2006).

We further validated these findings *in vivo* in a bacterial artificial chromosome (BAC) transgenic α-syn-GFP mouse model of PD pathogenesis previously establis-

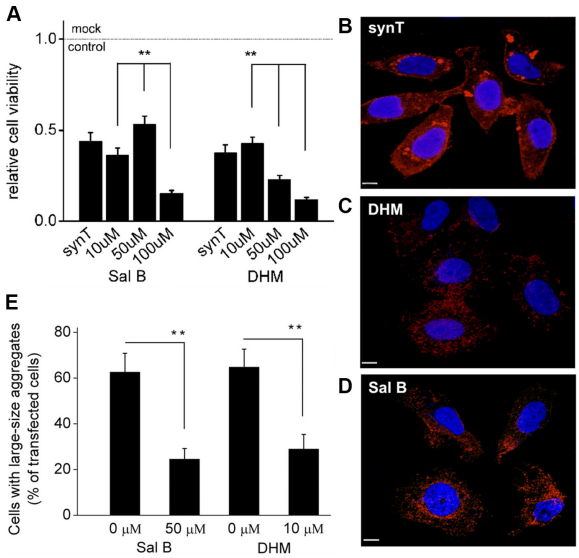

Figure 12 |Effect of DHM and SalB on α-synuclein aggregation. A) Assessment of cellular viability by MTT assay of H4 cells transfected with SynT and Synph-1, shows dose-dependent toxicity with increasing effects for both SalB and DHM. **B-D)** Immunostaining for α-synuclein aggregates in DHM (10 μM) or SalB (50 μM) treated H4 cells co-expressing SynT and Synph-1. A clearance of large aggregates were observed0. for compound-treated cells. **E)** Quantification of large aggregates in compound treated cells (B,C,D) reveal a significant decrease in aggregate quantity. (mean ± SD, *p<0.05, **p<0.01), Scale bar = 5 μm.

hed by our group (Hansen *et al.* 2013). Mice treated with either compound showed an increase in LAMP1 and LAMP2A immunoreactivity in the corpus striatum and the substantia nigra pars compacta (SNpc), similar to the levels seen in the cell-based model studies. Further examination of the brain tissue revealed a marked decrease in α-syn-GFP levels (Figure 13).

Taken together, these results highlight the value of reporter models for the study of α-syn biology, as well as in providing mechanistic insight on how potential therapeutic compounds may provide clearance of α-syn aggregation. A better understanding of the underlying molecular events observed here, could shape potential strategies in the prevention of α-syn aggregation.

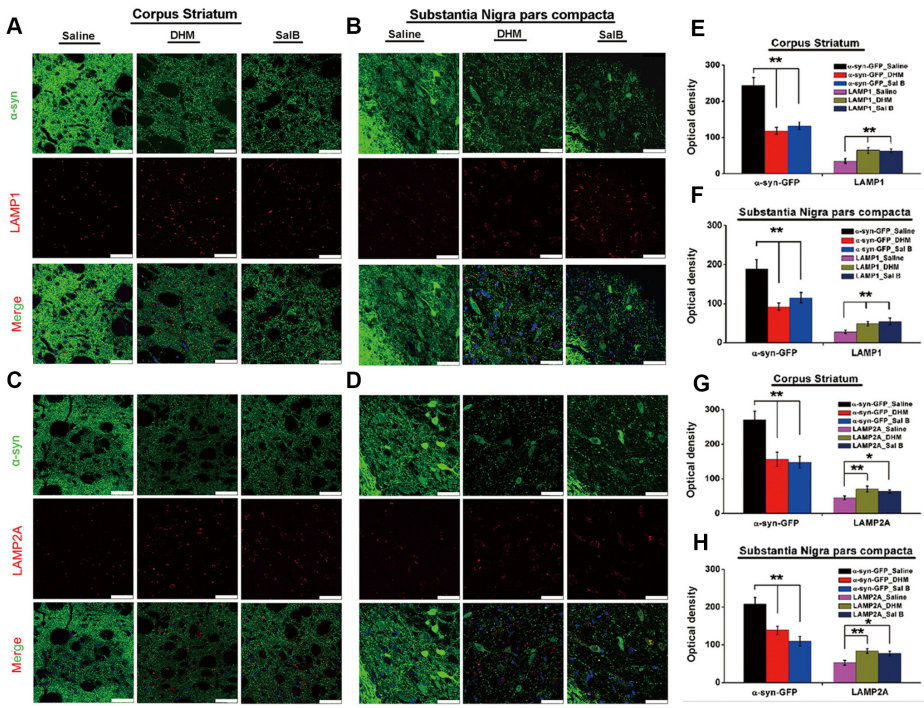

Figure 13 | Investigation of DHM and SalB effect on α-synuclein-GFP in mouse brain. Quantification of α-syn-GFP in the corpus striatum **(A, C)** and SNpc **(B, D)** of BAC-α-syn-GFP transgenic mice. Both DHM and SalB treated mice showed decreased abundance of α-synGFP, and an increased level of LAMP-1 and LAMP-2A in comparison with saline treated mice (8 animals/group, male). **E-H)** Quantification of optical density for α-synuclein-GFP, LAMP1 and LAMP2 for corresponding images. Significance given by (*p<0.05, **p<0.01) compared with the saline treatment. Scale bars = 50 µm.

Paper III

Establishing a HTS reporter model for α-synuclein pathology and its application in the investigation of underlying molecular mechanisms

Despite emerging knowledge of the pathogenic mechanisms driving neurodegenerative diseases in the last decade, there has been no clinical translation into disease-modifying therapies. One current approach to identifying new potential therapies is through compound screening. However, the attrition rates in such screens are very low, where only few potential candidates may arise from the millions of compounds originally screened. This discrepancy between the number of tested and approved drugs highlights the use for automated high-throughput screening (HTS) systems to address this unmet need. (Aldewachi *et al.* 2021)

With the aim of up-scaling the investigation of molecular events involved in α-syn pathology, we sought to develop a reporter system for α-syn aggregation with higher throughput potential. To this end, we selected a fluorescence resonance energy transfer (FRET)-based reporter system, previously characterised for detection of tau aggregation, a microtube-associated protein (MAP) also described to have aggregation propensity (Holmes *et al.* 2014; Sanders *et al.* 2014). This FRET biosensor is suitable for HTS screens due to its high sensitivity and potential for automation by flow cytometry (FC) (Holmes *et al.* 2014).

We generated a FRET-based α-syn aggregation reporter using the cyan and yellow fluorescent protein (CFP/YFP) FRET pair tethered to mutant α-synA53T similar to that reported by Diamond and colleagues (Yamasaki *et al.* 2019). The resulting reporter system develops large insoluble cytoplasmic aggregates which are FRET positive, allowing for robust detection of aggregate-containing cells by FC (Figure 14 A). This biosensor system displayed concentration-dependent sensitivity down to 90 ng/ml and 300ng/ml for lipofection-mediated transfection and direct addition of α-syn PFFs, respectively (Figure 14 B). Further examination of the induced aggregates showed them to exhibit traits associated with α-syn pathology such as p-α-Syn positivity, detergent insoluble α-syn and a cross-β-sheet structure (Figure 14 C-G).

Leveraging the sensitivity and scalability of our reporter model, we conducted a screen of small molecule kinase inhibitors to identify signalling pathways that

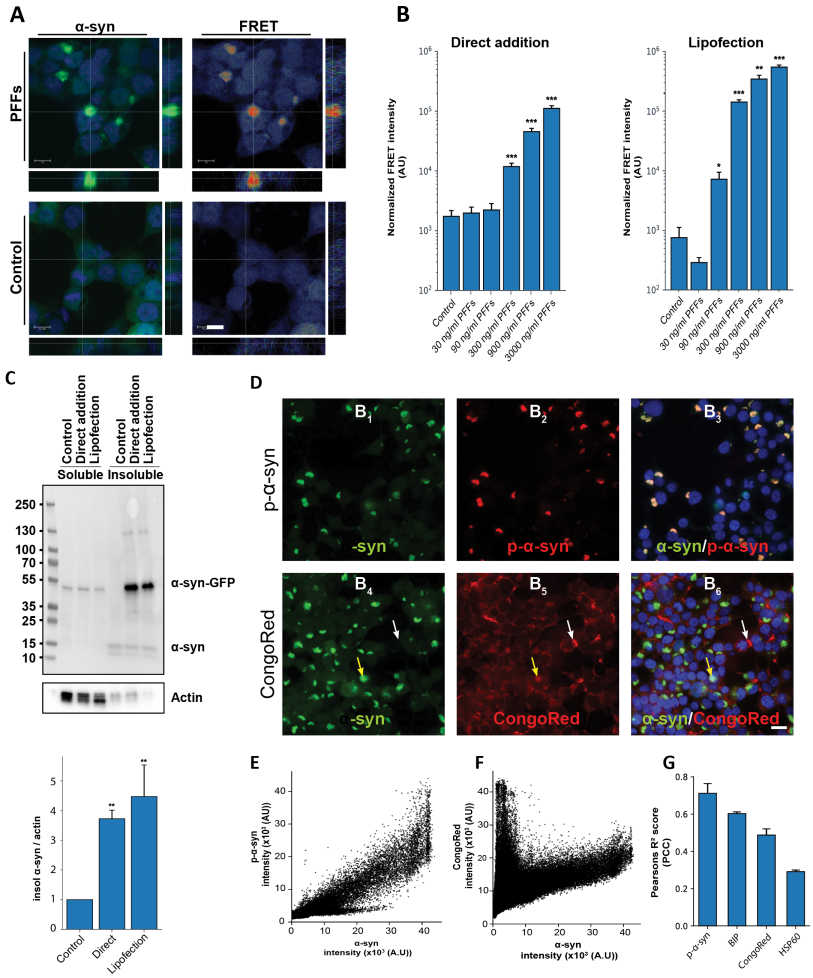

Figure 14| Generation and validation of a FRET-based α-synuclein aggregation reporter. A) Validation of FRET signal for induced aggregation in the biosensor cell line. Cells with aggregates show strong co-localized FRET signal, while no FRET is visible in absence of aggregates. **B)** Assessment of biosensor sensitivity for exogenously added PFFs. Direct addition (left) shows a significant detection of FRET signal at 300 ng/µl, while lipofection (right) shows significant detection at 90 ng/µl **C)** Both treatment with PFFs directly and by lipofection leads to formation of insoluble aggregates as seen by α-synuclein detection in the insoluble phase. **D)** Co-localization analysis of induced α-synuclein aggregates shown, GFP positive aggregates co-stain for p-α-synuclein and the cross-β specific dye CongoRed. (scale bar = 20 µm) **E)** Scatterplot to visualize co-localization between α-synuclein-GFP and p-α-synuclein. The diagonal spread of intensities indicate strong co-localization **F)** Similar to E, co-localization is visualized between α-synuclein-GFP and CongoRed. Two populations are visible, a strong CongoRed single staining and a double labelled CongoRed

and α-synuclein-GFP positive population **G)** PCC correlation scores between α-synuclein-GFP and the corresponding markers. Bar chart values show mean ± SD, *p < 0.05, **p < 0.005, ***p < 0.001. Statistical testing was performed using Brown–Forsythe and Welch one-way ANOVA for multiple comparisons to a control group

may be involved in α-syn pathology and potential inhibitors thereof. Out of 81 compounds screened, three inhibitors [GF109203X (GF), SB202190 (SB90) and SB203580 (SB80)] emerged as putative hit compounds, shown to have a potent impact on induced α-syn aggregation (Figure 15 A-B). Among the three hit compounds identified, two were inhibitors of p38 Mitogen-activated protein kinase (p38 MAPK; SB80 and SB90), and one inhibited protein kinase C (PKC; GF).

To assess their potential as therapeutic targets, we benchmarked our lead compounds against two other small molecule compounds [Enzastaurin (Enza) and VX-745 (VX)] which have recently been involved in clinical trials for other indications (Enza, Trial_ID: NCT03263026; and VX, Trial_ID: NCT02423200). These compounds have overlapping targets with the putative inhibitors identified, namely Enza and VX targeting PKC (Moreau *et al.* 2007) and p38 MAPK (Duffy *et al.* 2011), respectively. Upon conducting validations of the three hit compounds, we observe a robust protection against induced aggregation using both fluorescence microscopy and FC methodologies (Figure 15 C). Assessment of α-syn aggregation by FC revealed a significant reduction of FRET intensity for all compounds compared to vehicle-treated control (7.4-fold for GF, 12.4-fold for SB90 and 2.7-fold for SB80). Comparing the benchmarked compounds Enza and VX to our hit compounds, we observe a similar ability to prevent aggregation for Enza both by microscopy and FC. Interestingly, VX treatment instead trended towards a sensitization to α-syn aggregation, exhibiting comparable levels to the vehicle-treated cells (Figure 15 D).

Mass spectrometry (MS)-based phosphor-proteomics is becoming an essential methodology for the inference of kinase activity, as substrate phosphorylation status can serve as a comprehensive guide to understand cellular signalling involved (Savage and Zhang 2020). With the aim of delving into the dynamic changes in signalling networks prompted by the kinase inhibition, we examined the phosphor-proteomic landscape following treatments with all aforementioned inhibitors.

Unsupervised clustering of the subset from the phosphor-proteome that was significantly altered for all inhibitor-treated cells showed discrete profiles for each compound treatment. These unique profiles highlight the differences in the intrinsic signalling pathways affected even among inhibitors expected to have the same target (Figure 16 A). However, when comparing the global phosphor-proteome, similarities among inhibitors with the same target are more evident according to the inter-sample Pearson's correlation coefficient (PCC) (Figure 16 B).

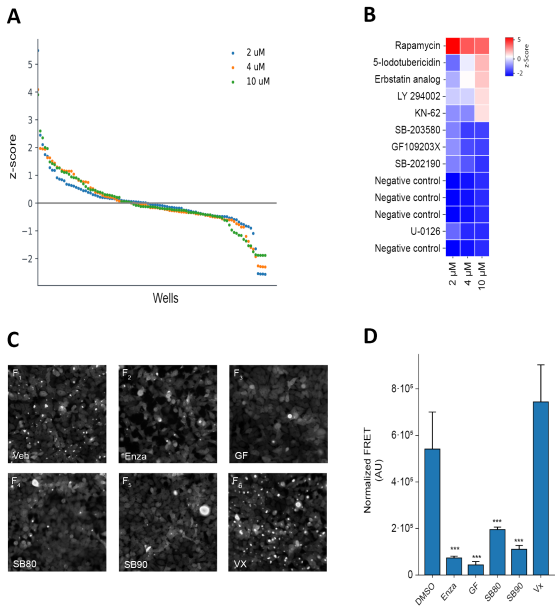

Figure 15 | Screening of kinase inhibitor library for modulators of α-synuclein aggregation. A) Outcome of screening a kinase inhibitor library in three inhibitor concentrations as measured by normalized FRET intensity for each well. Z-scores were calculated for each sample and the resulting output is seen to follow a waterfall distribution, with similar shapes across concentrations. **B)** Heatmap of samples with Z-scores >1.5 or <-1.5. Negative control samples are seen among the most negative Z-scores as expected. **C)** Biosensor cells treated with inhibitors and α-synuclein PFFs. Strong prevention of α-synuclein aggregation are observed for all samples except for vehicle and VX treatment. (Scale bar = 20 µm) **D)** Quantification of inhibitor effects by FRET-based FC shows significant protection against induced α-synuclein aggregation with the exception of VX treatment. Bar charts show mean ± SD, ***p < 0.001. Statistical testing was performed using one-way ANOVA with Dunnett's T3 post hoc test for multiple comparisons to a control group.

Deeper analysis of the phosphor-proteome allowed us to find annotated pathways that may be differentially regulated upon inhibitor treatment. Comparing against the annotated KEGG pathway database (Kanehisa and Goto 2000) we find the main enrichment/depletion signatures to be among RNA transport and spliceosome pathways (Figure 16 C). These changes indicate the differential effect induced by the inhibitors may lie at the translation level.

To examine if any changes were induced on the proteome, we also performed a proteomic analysis to assess protein abundance following treatment with the hit and benchmarked inhibitor-treated cells. As was observed in the phosphor-proteome,

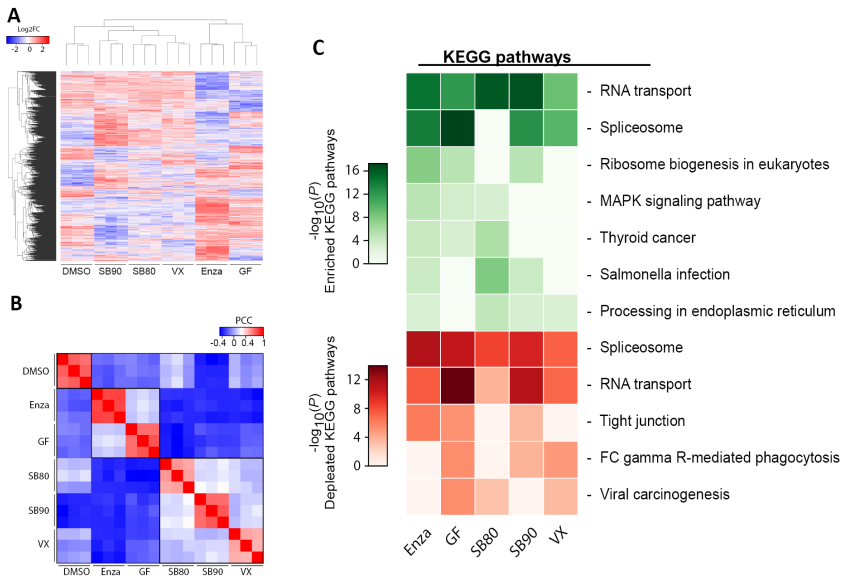

Figure 16 | Impact of hit compounds on phosphor-proteome. A) Unsupervised clustering of the significantly regulated phosphor-proteome reveal distinct patterns for each inhibitor. **B)** Pearsons correlation matrix reveals high sample similarity among replicates, but also similarity among inhibitors with the same target, although to a lower extent. **C)** By performing pathway analysis, we see spliceosome and RNA transport as being both most enriched and most depleted pathways in terms of phosphor-epitopes. This may indicate inhibitor-induced alterations can be found in the proteome.

the unsupervised clustering and PCC matrix showed distinct profiles and grouped compounds of similar targets together (Figure 17 A-B). Performing KEGG pathway analysis using the proteome data, we observe a depletion of proteins related to neurodegeneration-related pathways, such as those associated with PD, AD and Huntington's disease. This depletion largely stems from a decrease in mitochondrial proteins such as NDUF, COX and CYC which are shared among the annotated pathways (Figure 17 C).

While depletion in genes that map to these pathways may contribute to the prevention of aggregation, we found such changes absent for SB80 despite its anti-aggregation effects. Further, we see an enrichment in lysosomal-related proteins for all tested inhibitors except for VX, matching our expectation that all inhibitors effectively preventing α-syn aggregation will exhibit similar expression patterns (Figure 17 C).

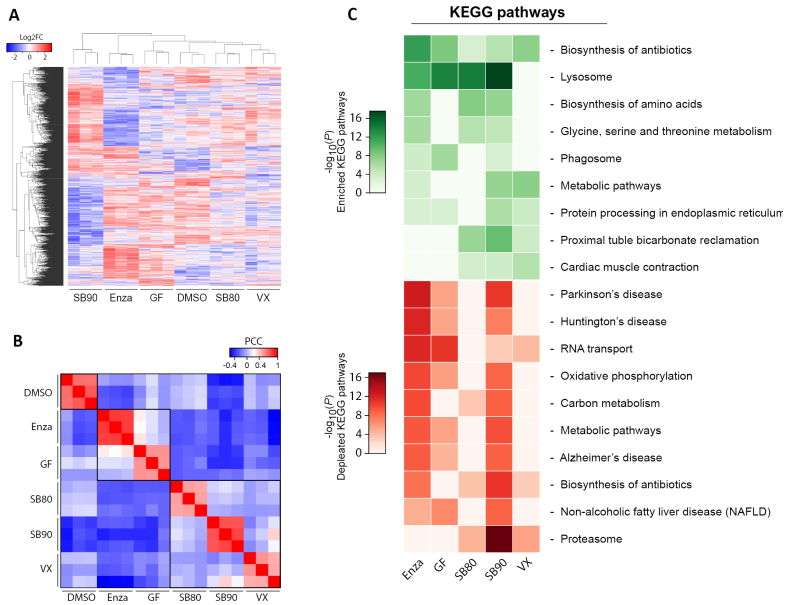

Figure 17 | Impact of hit compounds on proteome. A) Unsupervised clustering of the significantly regulated proteome reveal distinct patterns for each inhibitor. **B)** Pearsons correlation matrix reveals high sample similarity among replicates, and similar to the phosphor-proteome we also see similarity among inhibitors with the same target. **C)** By performing KEGG pathway analysis, we observe an enrichment in lysosome related proteins as mapped to the annotated lysosome pathway. Furthermore for Enza, GF and SB90 we also observe a depeltion in proteins related to the annotated pathways for Huntingtons disease, AD and PD.

Lysosomes are membrane-bound degradative compartments with the function of breaking down cellular components and maintaining cellular homeostasis. Given the enrichment seen in the lysosome-related proteins in the proteomic data, we visualized and quantified the relative abundance of lysosomes via live-cell microscopy and FC using LysoTracker. FC analysis revealed an increased abundance of lysosomes following treatment with GF, Enza and SB90, however not for SB80 and VX (Figure 18 A-B). As lysosomes are compartments in a constant flux, changes in abundance could come from either elevated biogenesis or decreased turnover. Quantification by microscopy of nuclear translocation of the master regulator of lysosomal biogenesis, transcription Factor EB (TFEB) (Malta *et al.* 2019), displayed no significant difference for any inhibitor treatment (Figure 18 C-D). TFEB regulates the expression of genes involved in different stages of the autophagy process, including genes involved in autophagy initiation, autophagosome trafficking,

substrate capture, and fusion with lysosomes (Palmieri *et al.* 2011; Settembre *et al.* 2011). The transcriptional activity of TFEB is largely regulated by subcellular localization. Upon dephosphorylation, TFEB translocates to the nucleus where it activates target genes (Malta *et al.* 2019). A lack of nuclear translocation of TFEB indicates TFEB-driven expression programs were not driving the increase in lysosomes, suggesting alterations may instead occur during endo-lysosomal maturation. FITC-dextran was used to monitor the rate of endocytic uptake by following FITC-

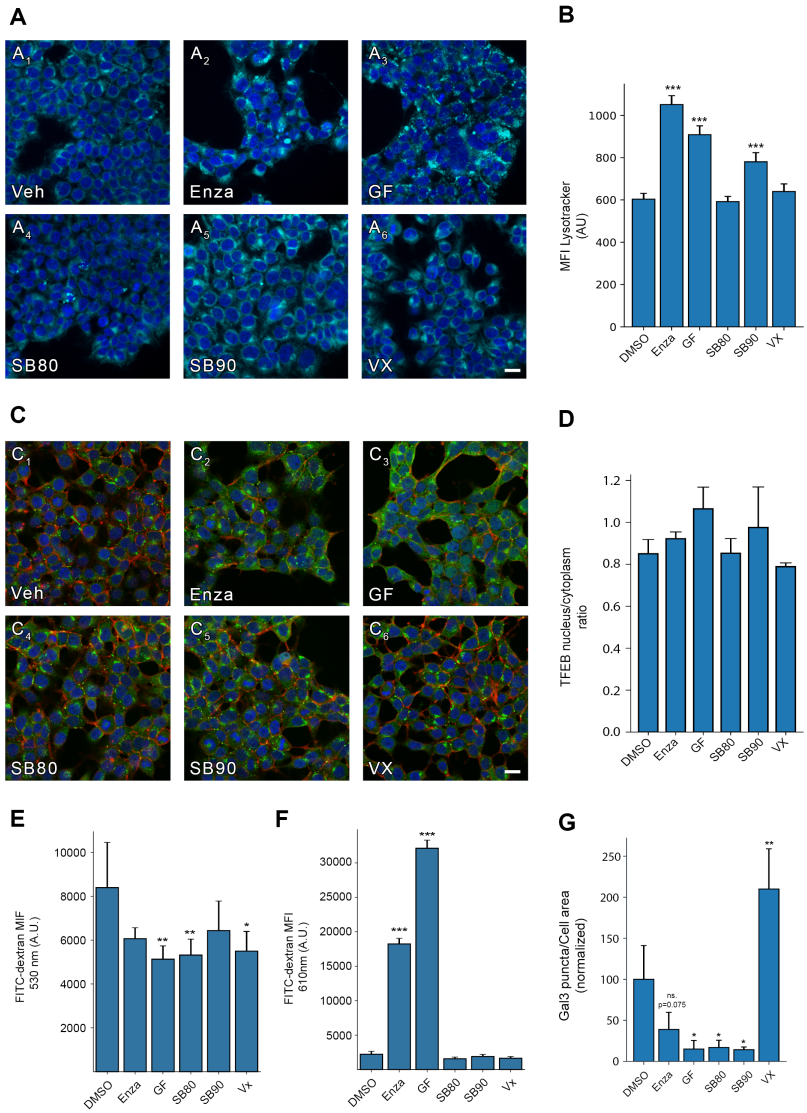

Figure 18 | Investigation of mechanisms involved in prevention of induced α-synuclein aggregation. A) Visualization of lysosomes in inhibitor-treated samples by staining with lysotracker. **B)** Quantification of lysotracker staining by FC reveals significantly elevated lysosome content for cells treated with Enza, GF and SB90. **C)** Investigation of nuclear translocation of Transcription Factor EB (TFEB), reveals no visible increase in nuclear localization. **D)** Automated image analysis confirms no significant translocation upon treatment with any inhibitor. **E)** Quantification of intracellular FITC-dextran by FC at 530 nm indicates a drop in FITC-dextran, but only accounts for non-quenched FITC-dextran. **F)** Quantification by FC of FITC-dextran at 610nm indicates an increased abundance of FITC-dextran inside cells treated with Enza and GF. **G)** Using a Gal3-GFP model for monitoring vesicular permeabilization, a significant drop in vesicle rupture was observed for GF, SB80 and SB90. Enza was found to have a trend toward a decrease but ultimately not significant. Instead a significant increase was observed for VX.). Bar chart values show MFI ± SD, *$p < 0.05$, **$p < 0.005$, ***$p < 0.001$. Statistical testing was performed using Brown–Forsythe and Welch one-way ANOVA for multiple comparisons to a control group. (Scale bar = 20 μm)

dextran loading into cells, but also to quantify lysosome-sequestered FITC-dextran. Following addition of FITC-dextran, we observed a significant decrease in internalized FITC-dextran for GF, SB80 and VX, but not for Enza and SB90 (Figure 18 E). That there is a decreased endocytic uptake following treatment with VX but no protection against induced aggregation indicates this drop in uptake would not explain the protection from the other compounds. Instead, when investigating the pH-insensitive tail-end of FITC's spectrum, we did observe a significant increase in intracellular FITC-dextran (Figure 18 F). Based on the signal only being present upon measuring the tail-end of the spectrum, we speculate the build-up of FITC-dextran must be in acidic compartments.

As the changes we observed were centered around lysosomal function, and a hypothesized route for a prion-like cell-to-cell spread is via endocytosis and subsequent cytosolic release (Freeman *et al.* 2013), we assessed the inhibitor effect on vesicular permeabilization. Using a galectin-3(Gal3)-GFP reporter cell line (Freeman *et al.* 2013), we show a significant reduction in vesicle permeabilization for all inhibitors, except for VX, which instead displayed a significant increase in the number of permeabilized vesicles present (Figure 18 G).

The findings reported here highlight the usefulness of developing FRET-based α-syn aggregation reporters in their application for semi-automated screening of compounds. Vast amounts of information can be leveraged from these screens in order to target key molecular events triggering α-syn aggregation.

Paper IV

Mapping the genetic landscape of induced α-synuclein aggregation

Investigations of molecular events are often complicated by the sheer number of concurrent processes ever ongoing inside a cell. This is also true for the study of human α-syn aggregation, especially as we are still far from understanding the numerous physiological functions it is involved in. One approach to elucidating the molecular processes driving aggregation is to map a reference protein-protein interactome as has been done for α-syn expressed in yeast (Chung *et al.* 2017). Studying the interaction of α-syn with target proteins on a large scale enables the identification of interconnected pathways implicated in synucleinopathies. We foresee an interactome map may aid the research community in discovering causal factors of PD pathogenesis.

We took a similar approach, utilizing our previously established FRET-based α-syn aggregation biosensor (Svanbergsson *et al.* 2021) to perform a genome-wide CRISPR knockout screen (Shalem *et al.* 2014). This FRET biosensor allows for an observable outcome of either presence or absence of α-syn aggregate content in our reporter HEK293T cells. Mapping single gene knockouts to the aggregation status allows us to bioinformatically assess which genes and gene networks may impact seeded α-syn aggregation.

For our genome-wide knockout screen, we selected the GeCKOv2 library, which targets 19.050 genes with approximately 6 guides per gene (Sanjana *et al.* 2014). Following sequential lentiviral transduction of the FRET biosensor cells with the sgRNA library and Cas9, we allowed the cells to expand for 72 hours to ensure gene knockout. The established cell-line maintained guide diversity at an average of ~94% coverage with minimal induced skew in representation (Figure 19 A-B).

To compare the impact of different protocols used for PFF production we included two α-syn PFFs generated by different protocols, here called PFF-A and PFF-B. In addition, we included two methods of aggregate induction: direct delivery of PFFs and lipofection. Each sample was FC sorted at endpoint based on FRET signal intensity to isolate aggregate-positive from aggregate-negative cells. SgRNAs were then amplified from genomic DNA and used to quantify recovery of cells with desired gene knockout.

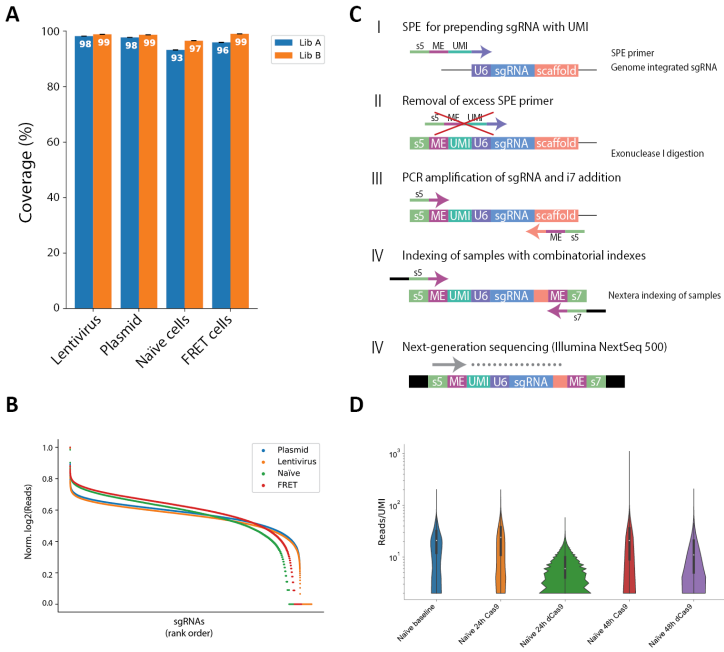

Figure 19 | Generation of sgRNA library containing biosensor cells and strategy for UMI tagging sgRNAs. A) Coverage of sgRNA pool for each cell cell line generated containing the GeCKO library. **B)** Abundance of each sgRNA for the generated cell lines shows a minimal increase in library skew from plasmid pool to stable cell line. **C)** Schematic overview of single primer extension. I) Target sgRNA is amplified in a single primer 1 cycle reaction for incorporation of a UMI. II) Excess unbound primer is degraded by exonuclease I. III) PCR amplification of sgRNA containing UMI. IV) Illumina indexing of sgRNA pool containing UMIs V) Illumina sequencing of sgRNA pool. **D)** Read counts of each UMI shows the uneven amplification by PCR. Each UMI is identified with 1-1000 reads.

A complication to bulk Illumina sequencing is the requirement for DNA pre-amplification of input samples. As PCR amplification does not yield a uniform amplification of all transcripts, a skew may be introduced during this step. Other modalities such as Drop-seq (Macosko *et al.* 2015) and other droplet-based single cell sequencing pipelines have resolved this issue by implementation of unique molecular identifiers (UMIs). These barcodes can be used to retrieve the transcript number in the original sample prior to amplification. Inspired by this approach, we applied a methodology called single primer extension (SPE) (Hoshino and Inagaki 2017) to add UMIs to each sgRNA prior to PCR as the first step in sample preparation (Figure 19 C). Obtaining UMI-labelled sgRNAs allowed us to correct

for amplification bias and boost the sensitivity and information content obtained from the pooled screen. With this correction, each sgRNA was only counted once, whereas the bulk data showed UMIs with read counts from 1-10^3 (Figure 19 D). However, the process only yielded us a low average recovery of 20.3% of the input cells. The loss of sgRNA representation at the UMI incorporation step, combined with a low inherent frequency of aggregates observed in control conditions, as well

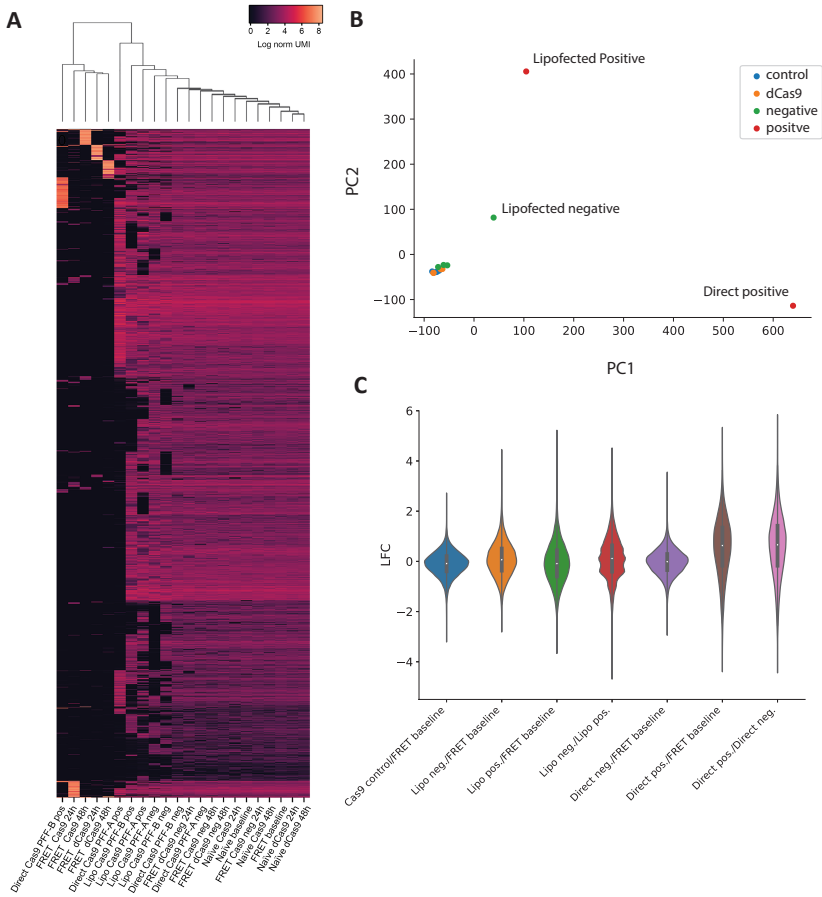

Figure 20 | Quality control and sample comparison of data from FC sorted samples. A) Unsupervised clustering of log normalized UMI counts from sequencing. Undersampled guides are evident by large blocks of absent data (black). **B)** Principle component analysis shows distinct grouping of samples. Control samples and aggregate-negative samples cluster together while aggregate-positive from PFF-treated samples separate from the main cluter. **C)** Distribution of sgRNA log2 fold change (LFC) between samples, show a normal distribution of LFCs. Comparing the aggregate positive samples with controls, we see a widening of the distribution indicating sgRNAs that undergo larger LFC.

as in the samples directly treated with the PFF-B strain, resulted in under sampling as seen by the sgRNA drop-out in black on the cluster map (Figure 20 A). As a result, only the most abundant sgRNAs were detected. Given the low percentage of mapped reads for the positive sorted fraction of control samples and PFF-B, we chose to only proceed with the analysis for samples treated with PFF-A.

Within the remaining samples, we find a clear clustering by 2D principal component analysis (PCA). Control samples were found to cluster tightly together, while three samples branched off from the main cluster (Figure 20 B). Among these

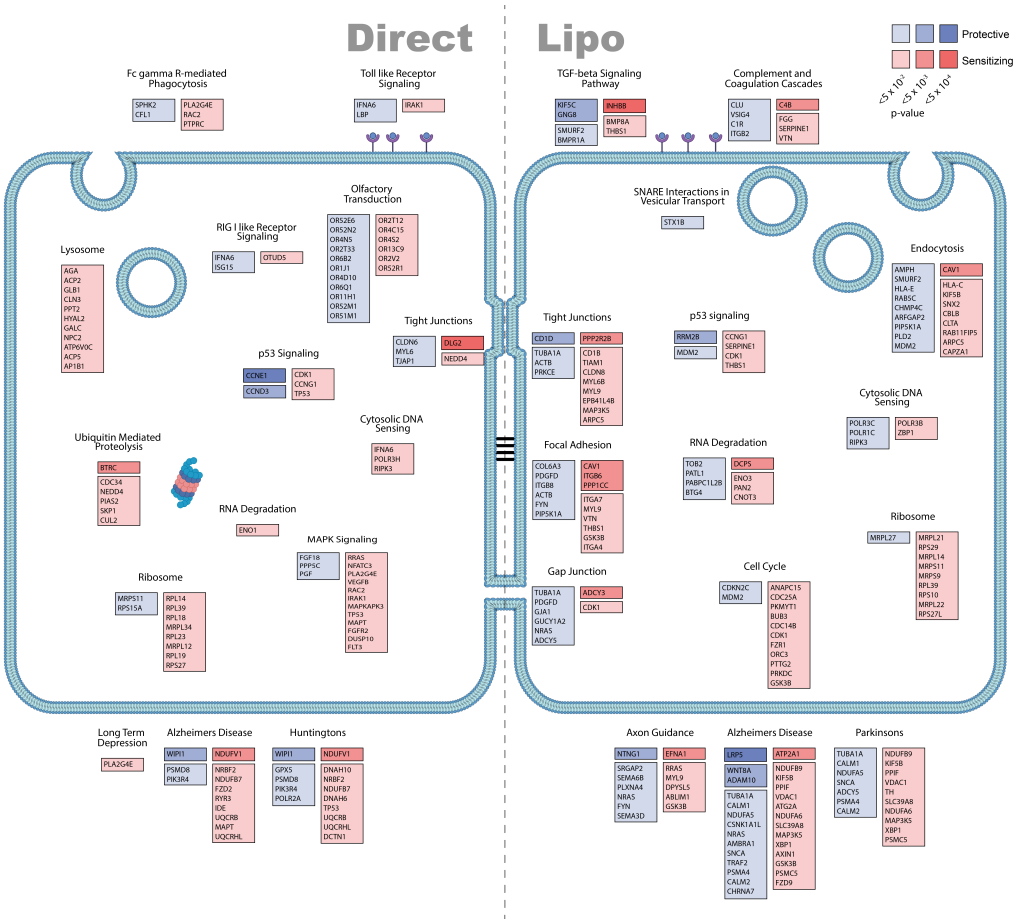

Figure 21 | Pathways with a significant impact on induced α-syn aggregation. Outcome of KEGG pathway analysis using the MaGECKs pathway analysis tool. The most altered pathways are illustrated with mapped genes displayed, with a minimum log2 fold change of 2 and p<0.05. (Red: Sensitizing; Blue: Protective)

three samples, aggregate-positive samples are at the extremes, while the aggregate-negative sample from the lipofection induction is closer to the control cluster.

Upon performing sample by sample comparisons we extract log2 fold change (LFC) and plot its distribution of sgRNA representation. We find most samples to be normally distributed around 0, indicating the vast majority of genes had little to no effect. This is especially true for control samples in absence of induced aggregation. With induced aggregation, we see a skew towards more extreme values in line with our expectation that more genes with larger differences could become evident during our screening condition of induced α-syn aggregation (Figure 20 C).

Based on the Model-based Analysis of Genome-wide CRISPR-Cas9 Knockout (MAGeCK) pathway analysis using the KEGG annotated pathway database, we identified pathways with a potential effect on α-syn aggregation, (Figure 21). Among these pathways we found well characterised pathways related to protein

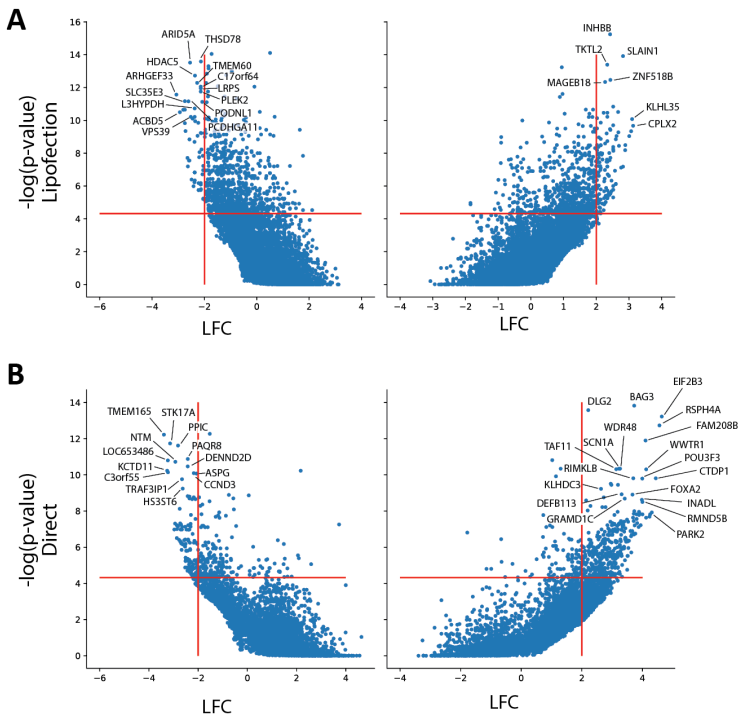

Figure 22 | Investigation of single gene impact on induced aggregation. A-B) Volano plots showing the LFC and signuificance of the observed impact on induced a-Syn aggregation. All genes included in the screen are dislplayed with gene labels showed for the most signficantly detected. Both Lipofection (A) and Direct addition (B) show distinct genes identified among enriched and dpleted fraction

quality control (lysosomal- and ubiquitin-mediated proteolysis) for samples treated with direct addition of PFFs. For the lipofection-treated samples, endocytosis and adhesion-related pathways emerge as significantly altered. Interestingly, we also find neurodegeneration-related signatures to be involved, such as PD, AD and Huntington's disease (Figure 21).

Notably, care must be taken when interpreting these prefixed datasets and making conclusions about causality of certain pathways on an aggregation phenotype. This might be the case for, either a gene that is significantly altered belonging to a pathway that is overall largely unchanged, or not annotated to any pathway dataset at all. We therefore also plotted the median LFC in sgRNA representation of differentially expressed genes in a volcano plot to identify strong modulators with a robust significance threshold (Figure 22). Among the top genes for the direct PFF addition we identified the parkin RBR E3 Ubiquitin Protein Ligase (*PARK2*), which is a known gene related to inheritable PD (Kitada *et al.* 1998). Taking a single gene analysis approach, we identify new interesting targets to investigate for their potential impact on α-syn aggregation. From the lipofection-treated samples, the genes identified are mainly related to vesicle trafficking, while for the direct PFFs addition, some interesting hits associated to translation machinery and protein quality control were detected (Figure 22). Functional experiments of candidate disease genes in *in vitro* and/or *in vivo* systems would then be needed to validate gene association to α-syn pathology.

In the present manuscript, we show the successful implementation of CRISPR/Cas9-based genome-wide knockout screening for the identification of modifiers of α-syn aggregation. Some findings reported here are well aligned with current knowledge of known modulators of α-syn pathology, confirming robustness of our screen. Notably, we identified several genes that could be potential new regulators of α-syn and may thus be unexplored dependencies of α-syn aggregation. Further examination and experimental validation of identified targets would help form a framework of molecular events involved.

Discussion and future perspectives

With the work presented in this thesis, we have sought to contribute to the understanding of the molecular mechanisms involved in synucleinopathy. In order to identify the molecular networks involved, our approach has been to model human PD pathology by perturbing α-syn aggregation through genetic or pharmacological ablation. To induce pathological features, we have relied on two distinct cell-based model systems: overexpression of mutant α-synA53T, and direct addition of α-syn PFFs.

To assess the pathological potential of both mutant α-syn and α-syn PFFs, we investigated their impact on primary murine hippocampal neurons. We found overexpression of WT α-syn to be well tolerated while A53T α-syn mutant lead to both NMDAR organisational and functional defects. Similarly, we found exogenous addition of α-syn PFFs induced comparable neuronal dysfunction. The observed dysregulation imparted on NMDAR in part resembles the pathological effects that may occur during synucleinopathy.

Having shown the pathological potential and implications of treatment with mutant α-syn and α-syn PFFs, we then proceeded to set up a model system to investigate the potential effects on α-syn aggregation of two compounds, DHM and SalB. While the compounds have been shown to be neuroprotective, their effect on α-syn was unknown. Using the transfection-based Synph-1/SynT aggregation reporter system, we showed a marked clearance of α-syn aggregates. The clearance correlated with a concomitant increase in markers for autophagy and CMA, suggestive of an involvement of degradative pathways. We further tested two compounds, DHM and SalB, known to exhibit neuroprotective effects. Both were found to clear aggregates in cell lines as well as reduce α-syn load and prevent neuronal loss in the transgenic BAC α-syn-GFP mouse model of PD.

Having successfully applied a cellular model to explore molecular events associated with the clearance of α-syn aggregation, we sought to scale up the throughput for such investigations. To this end, we developed a FRET-based α-syn aggregation reporter line in HEK293T capable of detecting down to ~6.5 nM α-syn PFF in a lipofection assay.

The relevance of the FRET reporter as a model system for α-syn pathology was consolidated as it recaptured a set of the most common features of α-syn pathology,

such as the development of insoluble α-syn aggregates which were phosphorylated and contained cross-β sheet structure as shown by CongoRed positive staining. By having a model that robustly recaptured α-syn aggregation traits, we were able to conduct a cell-based assay for HTS of a library of kinase inhibitors as a proof-of-concept. The screen resulted in three new compounds being identified, and highlighted PKC and p38 MAPK as potential targets to prevent α-syn pathology. These results, presented in paper III, show our model system works at scale and can identify both potential novel compounds but also lead to identification of molecular mechanisms at play in α-syn aggregation.

Given the successful implementation of the FRET aggregation reporter for compound screening, we employed the same cell reporter for a genome-wide CRISPR-Cas9 knockout screen consisting of a library targeting 19.050 genes. Compared to the compound screen, large scale genome-wide assays have a large potential to unlock insights into the mechanisms in α-syn aggregation. However, they also come with increased noise-to-signal ratios and generate complex datasets that are often difficult to analyse and interpret.

FRET-based reporter cells were transduced with the GeCKOv2 library to establish a stable cell line variant that maintained >90% of the original guide diversity. This retention allowed us to setup multiple simultaneous experimental conditions with a robust collective starting point. Indications of the validity of our approach was found in the differentially regulated pathways identified. For the lipofection-treated samples, knock down of endocytosis-related genes lead to protection against induced aggregation, in-line with uptake dependency for lipofection. For the samples exposed to direct PFF addition, we found, among other pathways, protein quality control-related pathways such as lysosomal and proteasomal pathways, of which their dysfunction has previously been tied to α-syn pathology. Computational analysis of the data from the screen identified a web of potentially implicated pathways and targets. While further functional validation of the targets is essential, our data highlights the potential of genome-wide screening as a tool for deciphering causal factors of synucleinopathies.

Future perspectives

Our understanding of α-syn aggregation has come a long way, based on the dedicated research over the past decades. The pace of research seems only to accelerate with the advent of next generation sequencing (NGS) and single cell sequencing, as they are paving the way for new avenues of research that have not been possible to pursue until now. Single cell sequencing and spatial transcriptomic methodologies allow us to investigate the transcriptomes and molecular changes at an unprecedented resolution and speed. A large part of molecular biological research is likely to benefit from such methodological advances, especially as they become more broadly available as the price drops with the broader implementation.

To ensure we can take advantage of the technologies that become available, there will be an increasing need for computational analysis of large-scale datasets. Such datasets will however also allow us to answer our research questions at much-refined scale and larger scope. With such advances and a good implementation, we will have the tools to build an understanding of the pathological changes occurring in synucleinopathies, and potentially design disease-modifying treatments in the near future.

Key methods

Molecular methods

Gibson cloning

Gibson cloning was applied as the main method for construct generation due to its scarless DNA assembly, ease of planning, high efficiency and low background. For all Gibson assemblies performed throughout the work presented here, the clonings were planned using the online tool provided by New England Biolabs, NEBuilder.

For all planned clonings we used restriction digest, with Fermentas FastDigest enzymes, to linearize the vector backbone. Linearized backbones were gel purified and isolated using Zymo Gel DNA recovery kits. Inserts were prepared by PCR amplification using guides designed with NEBuilder and Phusion Hotstart II DNA polymerase 2xMasterMix. PCR reactions were composed of 25 µl Phusion Hotstart II 2xMasterMix, 1 µl forward primer (10 µM), 1 µl reverse primer (10 µM), 5 ng template DNA and water to 50 µl total reaction volume. Thermo cycling was performed by standard protocol: 3 min initial denature at 95 °C, 30 cycles (15 sec. denature at 95 °C, 20 sec primer-specific annealing temp., and 1min/kb at 72 °C for extension) and a further 5 min final extension at 72 °C. PCR product was then purified on an agarose gel and recovered by Zymo Gel DNA recovery kit.

Purified vector backbone (50 ng) and insert (2x molar excess) was then used in an isothermal Gibson reaction (New England Biolabs) at 50 °C for 1 hour. Resultant ligation mix was then transformed into Shure2 competent cells to identify positive colonies.

Single Primer Extension

For SPE we designed a primer with a binding sequence complimentary to the U6 promoter, with an overhang containing a 5xVHDB motif and a s5 and ME sequence at the opposing terminal. The semi-random nature of the 5xVHDB domain allows us to use it as a UMI while the s5/ME sequence facilitates downstream indexing of amplified reads.

SPE was performed using isolated genomic DNA from cells harbouring stable integrations of sgRNAs. UMI incorporation was facilitated by a single cycle of 2 min at 95 °C for denaturing, ramping to 68 °C with 0.3 °C/s and elongated for 20 min at 72 °C using Phusion Hotstart II 2xMM. Excess SPE primer was degraded by adding 1 µl exonuclease I and incubating for 20 min at 37 °C followed by heat inactivation for 20 min at 80 °C. The resultant reaction contains sgRNA with prepended UMI, which can selectively be amplified by Nextera indexing primers.

Soluble insoluble western blotting

Separation of soluble and insoluble protein fractions from cultured cells was performed through sequential extraction. First, cells were harvested in cold lysis buffer (20 mM Trizma base, 150 mM NaCl, 1 mM EDTA, 0.25% NP-40, 0.25% Triton-X-100) supplemented with protease and phosphatase inhibitors. Lysis was carried out for 20 min on ice, and the resulting lysate was spun for 20 min at 4 °C, 14.000g to pellet insoluble material. The supernatant makes out the detergent soluble fraction and was collected. The pellet was resuspended in lysis buffer containing 5% (w/v) SDS and following sonicated by cup-horn at 60% amplitude, 3 second pulses for 15 seconds. The resuspended pellet forms the detergent insoluble fraction.

Western blotting (WB) was performed by separating equal amounts of protein on a precast 4-15% Bis-Tris polyacrylamide gels. Using a BioRad Trans-Blot semidry transfer system, proteins were transferred to nitrocellulose membranes. Membranes were then blocked for 1 hour in PBS with 0.1% tween-20 and 3 % BSA. Blots were then probed with antibodies of choice.

Immunocytochemistry

To fix cells for immunostaining, 1 well volume of 8% PFA was added to the culture well (4% final concentration) at experimental endpoint. Cells were fixed for 15 min at room temperature before PFA was removed and cells were gently washed 3 times with PBS.

Fixed cells were blocked and permeabilized by incubation with PBS+0.1% Tween-20 (PBS-T) +1% BSA for 1 hour at room temperature. Following permeabilization,

the cells were washed 3 times for 5 minutes with PBS, before incubating with primary antibody in PBS-T+1% BSA at 4 °C over night.

Primary antibody was removed by 3 washes of 5 minutes with PBS before incubating with secondary antibody in PBS-T+1% BSA for 1 hour at room temperature. Last, cells were washed 3 times for 5 min with PBS before imaging.

Lentivirus production

Production of lentivirus throughout this thesis have has on 3rd generation lentiviral vectors, where necessary components for viral assembly is split into three support plasmids. Production was carried out by PEI based transfection in HEK293T cells as described below.

The day prior to initiation of virus production, $12.5x10^6$ HEK293T cells were seeded in a T175 flask to achieve an 85-90% confluence the following day. On the following day, culture medium was replaced 1 hour prior to transfection. DNA was prepared by diluting 5.1µg pMD2G, 7.1 µg pMDL and 4 µg pRsvRev along with 18 µg lentiviral vector plasmid in 1.7 ml OPTI-MEM and mixed by vortex. Liposomes were assembled by adding 102.6 µg PEI to diluted DNA, vortexed thoroughly and incubated for 15 min at RT prior to addition to cells for transfection.

Cell supernatant containing lentivirus was collected 48 hours after transfection and spun at 800xg for 10 min to remove cell debris and filtered through a 0.45 µm syringe filter. Lentivirus containing supernatant was further concentrated by ultracentrifugation for 1.5 hours, 107000xg at 4 °C. Pelleted lentivirus was resuspended over night at 4 °C in PBS to yield final lentivirus preparation.

Lentivirus titration

To assess lentiviral titre, a reference batch of lentivirus was established with GFP-driven by eIF1α. The reference batch titre was functionally assessed by FC.

Subsequent lentiviral preparations were then compared by qPCR based on WPRE integrations to the reference batch to determine titre. Briefly, HEK293T cells were seeded at 100.000 cells/well in a 6 well plate and incubated at 37 °C to allow sedimentation and adherence. Seeded cells were then transduced with 0.3 µl, 1 µl or 3 µl virus preparation. After 72 hours incubation at standard conditions, genomic DNA was extracted by Qiagen DNeasy Blood & Tissue kit. Viral integration was quantified by qPCR using self-quenching FAM probes for WPRE and albumin. Quantification was then performed using the ΔΔCT method using WPRE for viral integrations and albumin as control for cell numbers.

Production of recombinant α-synuclein

To produce monomeric α-syn, *E. coli* were transformed with an inducible pET3a plasmid containing human α-syn cDNA. Transformed bacteria were grown at 37 °C with 125 rpm shaking until OD600 of 0.6-1 is reached. Induction of α-syn expression was performed by addition of IPTG at 0.4mM final concentration for 4 hours. Crude α-syn was extracted by pelleting bacteria, followed by heat treatment and ion exchange chromatography. Prior to further purification, the crude α-syn was lyophilized and resuspended in the desired end buffer. Resultant α-syn was further purified by size exclusion chromatography on a Superdex 75 column in the desired end buffer. To isolate monomers, the corresponding monomer peak was collected and quantified by Nanodrop.

Production of α-synuclein PFFs

Purified α-syn monomers in Tris buffer (10 mM Tris, 150 mM NaCl, pH 7.5) at a concentration of 0.5 μg/μl were incubated for 14 days at 37 °C under 1000 rpm shaking using a 3 mm magnetic stir-bar. Fibrillation was followed by separate readings of Thioflavin T fluorescence in a control well to ensure plateau was reached. Formed PFFs were collected, aliquoted and stored at -80 °C until use.

α-synuclein kinetics assay

Aggregation kinetics was assessed in a 96 well plate format with 70 μM α-syn monomers with 20 μM thioflavin T for measuring aggregate content. Each compound reaction was prepared with wells with proportional volume of DMSO as vehicle. Initiation of the assay was performed by adding 0.1% molar concentration of α-syn PFF seeds. α-syn seeds were freshly sonicated prior to addition to the reaction well. Kinetics of the aggregation reactions was assessed on a BMG FLUOstar Omega plate reader at quiescently at 37 °C. An initial baseline of 3 hours was acquired before seed addition, after which readings were continuously performed for 12 hours.

In vitro

Cell culture

Mammalian cells were cultured at 37 °C, 95% relative humidity and 5% CO_2. Cells were maintained in DMEM supplemented with 10% FBS and 1% penicillin and streptomycin. Subculturing was performed by gentle mechanical detachment at ~80% confluency to maintain cells in constant growth phase. To seed cells for experimental conditions, cells were harvested with trypsin to ensure a single cell suspension and pelleted to remove trypsin. Cells were then counted and seeded at either 30.000 cells/cm^2 for direct addition experiments with PFFs or 90.000 cells/cm^2 for lipofection.

Generation of stable cell lines

To generate monoclonal stable cell lines, the parental cell line was seeded in a multi-well plate and transduced with lentivirus encoding the desired transgene. Following 6 days of continuous expansion, cells were harvested with trypsin and resuspended in PBS supplemented with 2% FBS. Transduced cell suspension was then sorted as single cells on a FACS Aria III equipped with a 100 µM nozzle, into a 96 well plate. Sorted single cells were then expanded until formation of a stable cell line.

Induction of α-synuclein aggregation

Addition of aggregation by PFF addition was performed with sonicated fibrils. Sonication was performed using a cup-horn sonicator at 60% amplitude in 3 sec on/off cycles for 15 sec. All PFFs were sonicated immediately before use.

For direct addition 30.000 cells/cm^2 were seeded the day prior. The next day, to induce aggregation, sonicated PFFs were added directly to the culture medium.

For lipofection, cells were seeded at a density of 90.000 cells/cm^2 the day prior. Next day, lipofection reaction was prepared by combining 1 µl lipofectamine 2000 with 9 µl OPTI-MEM and mixed well before 5 min incubation at room temperature. Liposomes were then mixed with freshly sonicated PFFs and incubated a further 10 min. Liposome and PFF complexes were then added to the culture wells to facilitate induction of aggregation.

Vesicular permeabilization assay

To monitor vesicular permeabilization, we used a previously developed Galectin3-GFP expressing HEK293T reporter line. Cells were seeded at a density of 20.000 cells/well in a 96 well plate. The following day, direct addition of α-syn was performed as previously described. 24 hours after addition of α-syn PFFs, cells were fixed and imaged to quantify puncta formation.

FRET based flow cytometry

For analysis of FRET intensities by FC, all cells were fixed in suspension. To suspension-fix cells, they were harvested at endpoint by trypsin, transferred to DMEM +10%FBS +1% P/S and centrifuged at 800g for 10 min to pellet. The pellet was resuspended in 100 µl PBS to which 100 µl 4% PFA was added (2% final concentration). Cells were fixed on ice with shaking every 5 min for 20 min. Fixed cells were then washed 3 times in PBS prior to analysis on a BD LSRFortessa. To detect FRET signal, a scatterplot of CFP vs FRET was setup by exciting with the 405 nm laser and emission collected at a decector equipped with 405/50 nm and 525/50 nm filter, respectively. To quantify FRET intensity we calculated the normalized FRET score (% FRET+ x FRET mean fluorescence intensity).

References

Alderson TR, Bax A (2016) Disorder in the court. Nature 530:38–39. https://doi.org/10.1038/nature16871

Aldewachi H, Al-Zidan RN, Conner MT, Salman MM (2021) High-Throughput Screening Platforms in the Discovery of Novel Drugs for Neurodegenerative Diseases. Bioeng 8:30. https://doi.org/10.3390/bioengineering8020030

Alvarez-Erviti L, Seow Y, Schapira AH, *et al* (2011) Lysosomal dysfunction increases exosome-mediated α-synuclein release and transmission. Neurobiol Dis 42:360–367. https://doi.org/10.1016/j.nbd.2011.01.029

Angot E, Steiner JA, Tomé CML, *et al* (2012) α-Synuclein Cell-to-Cell Transfer and Seeding in Grafted Dopaminergic Neurons *In Vivo*. Plos One 7:e39465. https://doi.org/10.1371/journal.pone.0039465

Arnaoutoglou NA, O'Brien JT, Underwood BR (2019) Dementia with Lewy bodies — from scientific knowledge to clinical insights. Nat Rev Neurol 15:103–112. https://doi.org/10.1038/s41582-018-0107-7

Atsushi T, Takafumi H, Michiko M-K, *et al* (2006) Mechanisms of Neuronal Death in Synucleinopathy. Biomed Res Int 2006:19365. https://doi.org/10.1155/jbb/2006/19365

Bartels T, Choi JG, Selkoe DJ (2011) α-Synuclein occurs physiologically as a helically folded tetramer that resists aggregation. Nature 477:107–110. https://doi.org/10.1038/nature10324

Blum D, Torch S, Lambeng N, *et al* (2001) Molecular pathways involved in the neurotoxicity of 6-OHDA, dopamine and MPTP: contribution to the apoptotic theory in Parkinson's disease. Prog Neurobiol 65:135–172. https://doi.org/10.1016/s0301-0082(01)00003-x

Bodner RA, Outeiro TF, Altmann S, *et al* (2006) Pharmacological promotion of inclusion formation: A therapeutic approach for Huntington's and Parkinson's diseases. P Natl Acad Sci Usa 103:4246–4251. https://doi.org/10.1073/pnas.0511256103

Bousset L, Pieri L, Ruiz-Arlandis G, *et al* (2013) Structural and functional characterization of two α-synuclein strains. Nat Commun 4:2575. https://doi.org/10.1038/ncomms3575

Braak H, Ghebremedhin E, Rüb U, *et al* (2004) Stages in the development of Parkinson's disease-related pathology. Cell Tissue Res 318:121–134. https://doi.

org/10.1007/s00441-004-0956-9

Braak H, Rüb U, Gai WP, Tredici KD (2003) Idiopathic Parkinson's disease: possible routes by which vulnerable neuronal types may be subject to neuroinvasion by an unknown pathogen. J Neural Transm 110:517–536. https://doi.org/10.1007/s00702-002-0808-2

Brettschneider J, Suh E, Robinson JL, *et al* (2018) Converging Patterns of α-Synuclein Pathology in Multiple System Atrophy. J Neuropathology Exp Neurology 77:1005–1016. https://doi.org/10.1093/jnen/nly080

Burré J (2015) The Synaptic Function of α-Synuclein. J Park Dis 5:699–713. https://doi.org/10.3233/jpd-150642

Campioni S, Bagnani M, Pinotsi D, *et al* (2020) Interfaces Determine the Fate of Seeded α-Synuclein Aggregation. Adv Mater Interfaces 7:2000446. https://doi.org/10.1002/admi.202000446

Campioni S, Carret G, Jordens S, *et al* (2014) The Presence of an Air–Water Interface Affects Formation and Elongation of α Synuclein Fibrils. J Am Chem Soc 136:2866–2875. https://doi.org/10.1021/ja412105t

Chang J-W, Wachtel SR, Young D, Kang U-J (1999) Biochemical and anatomical characterization of forepaw adjusting steps in rat models of Parkinson's disease: studies on medial forebrain bundle and striatal lesions. Neuroscience 88:617–628. https://doi.org/10.1016/s0306-4522(98)00217-6

Chartier S, Duyckaerts C (2018) Is Lewy pathology in the human nervous system chiefly an indicator of neuronal protection or of toxicity? Cell Tissue Res 373:149–160. https://doi.org/10.1007/s00441-018-2854-6

Chung CY, Khurana V, Yi S, *et al* (2017) *In Situ* Peroxidase Labeling and Mass-Spectrometry Connects α-Synuclein Directly to Endocytic Trafficking and mRNA Metabolism in Neurons. Cell Syst 4:242-250.e4. https://doi.org/10.1016/j.cels.2017.01.002

Danzer KM, Kranich LR, Ruf WP, *et al* (2012) Exosomal cell-to-cell transmission of α-synuclein oligomers. Mol Neurodegener 7:42. https://doi.org/10.1186/1750-1326-7-42

Delenclos M, Burgess JD, Lamprokostopoulou A, *et al* (2019) Cellular models of α-synuclein toxicity and aggregation. J Neurochem 150:566–576. https://doi.org/10.1111/jnc.14806

Dettmer U, Newman AJ, Saucken VE von, *et al* (2015a) KTKEGV repeat motifs are key mediators of normal α-synuclein tetramerization: Their mutation causes excess monomers and neurotoxicity. Proc National Acad Sci 112:9596–9601. https://doi.org/10.1073/pnas.1505953112

Dettmer U, Newman AJ, Soldner F, *et al* (2015b) Parkinson-causing α-synuclein missense mutations shift native tetramers to monomers as a mechanism for disease

initiation. Nat Commun 6:7314. https://doi.org/10.1038/ncomms8314

Dickson DW (1999) Tau and Synuclein and Their Role in Neuropathology. Brain Pathol 9:657–661. https://doi.org/10.1111/j.1750-3639.1999.tb00548.x

Duffy JP, Harrington EM, Salituro FG, *et al* (2011) The Discovery of VX-745: A Novel and Selective p38α Kinase Inhibitor. Acs Med Chem Lett 2:758–763. https://doi.org/10.1021/ml2001455

Duffy PE, Tennyson VM (1965) Phase and Electron Microscopic Observations of Lewy bodies and Melanin Granules in the Substantia Nigra and Locus Caeruleus in Parkinson's disease. J Neuropath Exp Neur 24:398–414. https://doi.org/10.1097/00005072-196507000-00003

Durante V, Iure A de, Loffredo V, *et al* (2019) α-synuclein targets GluN2A NMDA receptor subunit causing striatal synaptic dysfunction and visuospatial memory alteration. Brain 142:1365–1385. https://doi.org/10.1093/brain/awz065

Emanuele M, Esposito A, Camerini S, *et al* (2016) Exogenous α-Synuclein Alters Pre- and Post-Synaptic Activity by Fragmenting Lipid Rafts. Ebiomedicine 7:191–204. https://doi.org/10.1016/j.ebiom.2016.03.038

Engelhardt E, Gomes M da M (2017) Lewy and his inclusion bodies: Discovery and rejection. Dementia Neuropsychologia 11:198–201. https://doi.org/10.1590/1980-57642016dn11-020012

Eskelinen E-L (2006) Roles of LAMP-1 and LAMP-2 in lysosome biogenesis and autophagy. Mol Aspects Med 27:495–502. https://doi.org/10.1016/j.mam.2006.08.005

Falcon B, Zhang W, Murzin AG, *et al* (2018a) Structures of filaments from Pick's disease reveal a novel tau protein fold. Nature 561:137–140. https://doi.org/10.1038/s41586-018-0454-y

Falcon B, Zhang W, Schweighauser M, *et al* (2018b) Tau filaments from multiple cases of sporadic and inherited Alzheimer's disease adopt a common fold. Acta Neuropathol 136:699–708. https://doi.org/10.1007/s00401-018-1914-z

Falcon B, Zivanov J, Zhang W, *et al* (2019) Novel tau filament fold in chronic traumatic encephalopathy encloses hydrophobic molecules. Nature 568:420–423. https://doi.org/10.1038/s41586-019-1026-5

Fernández RD, Lucas HR (2018) Isolation of recombinant tetrameric N-acetylated α-synuclein. Protein Expres Purif 152:146–154. https://doi.org/10.1016/j.pep.2018.07.008

Ferreira DG, Temido-Ferreira M, Miranda HV, *et al* (2017) α-synuclein interacts with PrPC to induce cognitive impairment through mGluR5 and NMDAR2B. Nat Neurosci 20:1569–1579. https://doi.org/10.1038/nn.4648

Fitzpatrick AWP, Falcon B, He S, *et al* (2017) Cryo-EM structures of tau filaments from Alzheimer's disease. Nature 547:185–190. https://doi.org/10.1038/nature23002

Flower TR, Chesnokova LS, Froelich CA, *et al* (2005) Heat Shock Prevents α-synuclein-induced Apoptosis in a Yeast Model of Parkinson's Disease. J Mol Biol 351:1081–1100. https://doi.org/10.1016/j.jmb.2005.06.060

Freeman D, Cedillos R, Choyke S, *et al* (2013) α-Synuclein Induces Lysosomal Rupture and Cathepsin Dependent Reactive Oxygen Species Following Endocytosis. Plos One 8:e62143. https://doi.org/10.1371/journal.pone.0062143

George JM (2001) The synucleins. Genome Biol 3:reviews3002.1. https://doi.org/10.1186/gb-2001-3-1-reviews3002

Glajch KE, Moors TE, Chen Y, *et al* (2021) Wild-type GBA1 increases the α-synuclein tetramer–monomer ratio, reduces lipid-rich aggregates, and attenuates motor and cognitive deficits in mice. Proc National Acad Sci 118:e2103425118. https://doi.org/10.1073/pnas.2103425118

Golbe LI, Lazzarini AM, Duvoisin RC, *et al* (1996) Clinical genetic analysis of Parkinson's disease in the contursi kindred. Ann Neurol 40:767–775. https://doi.org/10.1002/ana.410400513

Greten-Harrison B, Polydoro M, Morimoto-Tomita M, *et al* (2010) αβγ-Synuclein triple knockout mice reveal age-dependent neuronal dysfunction. Proc National Acad Sci 107:19573–19578. https://doi.org/10.1073/pnas.1005005107

Griffioen G, Duhamel H, Damme NV, *et al* (2006) A yeast-based model of α-synucleinopathy identifies compounds with therapeutic potential. Biochimica Et Biophysica Acta Bba - Mol Basis Dis 1762:312–318. https://doi.org/10.1016/j.bbadis.2005.11.009

Guo M, Wang J, Zhao Y, *et al* (2020) Microglial exosomes facilitate α-synuclein transmission in Parkinson's disease. Brain 143:1476–1497. https://doi.org/10.1093/brain/awaa090

Halliday GM (2015) Re-evaluating the glio-centric view of multiple system atrophy by highlighting the neuronal involvement. Brain 138:2116–2119. https://doi.org/10.1093/brain/awv151

Hansen C, Björklund T, Petit GH, *et al* (2013) A novel α-synuclein-GFP mouse model displays progressive motor impairment, olfactory dysfunction and accumulation of α-synuclein-GFP. Neurobiol Dis 56:145–155. https://doi.org/10.1016/j.nbd.2013.04.017

Harms AS, Kordower JH, Sette A, *et al* (2021) Inflammation in Experimental Models of α-Synucleinopathies. Movement Disord 36:37–49. https://doi.org/10.1002/mds.28264

Holmes BB, Furman JL, Mahan TE, *et al* (2014) Proteopathic tau seeding predicts tauopathy *in vivo*. Proc National Acad Sci 111:E4376–E4385. https://doi.org/10.1073/pnas.1411649111

Holmqvist S, Chutna O, Bousset L, *et al* (2014) Direct evidence of Parkinson patholo-

gy spread from the gastrointestinal tract to the brain in rats. Acta Neuropathol 128:805–820. https://doi.org/10.1007/s00401-014-1343-6

Hoshino T, Inagaki F (2017) Application of Stochastic Labeling with Random-Sequence Barcodes for Simultaneous Quantification and Sequencing of Environmental 16S rRNA Genes. Plos One 12:e0169431. https://doi.org/10.1371/journal.pone.0169431

Jahn TR, Makin OS, Morris KL, *et al* (2010) The Common Architecture of Cross-β Amyloid. J Mol Biol 395:717–727. https://doi.org/10.1016/j.jmb.2009.09.039

Kanehisa M, Goto S (2000) KEGG: Kyoto Encyclopedia of Genes and Genomes. Nucleic Acids Res 28:27–30. https://doi.org/10.1093/nar/28.1.27

Kim S, Yun SP, Lee S, *et al* (2018) GBA1 deficiency negatively affects physiological α-synuclein tetramers and related multimers. Proc National Acad Sci 115:798–803. https://doi.org/10.1073/pnas.1700465115

Kirik D, Rosenblad C, Burger C, *et al* (2002) Parkinson-Like Neurodegeneration Induced by Targeted Overexpression of α-Synuclein in the Nigrostriatal System. J Neurosci 22:2780–2791. https://doi.org/10.1523/jneurosci.22-07-02780.2002

Kitada T, Asakawa S, Hattori N, *et al* (1998) Mutations in the parkin gene cause autosomal recessive juvenile parkinsonism. Nature 392:605–608. https://doi.org/10.1038/33416

Kordower JH, Chu Y, Hauser RA, *et al* (2008) Lewy body–like pathology in long-term embryonic nigral transplants in Parkinson's disease. Nat Med 14:504–506. https://doi.org/10.1038/nm1747

Kosaka K, Yoshimura M, Ikeda K, Budka H (1984) Diffuse type of Lewy body disease: progressive dementia with abundant cortical Lewy bodies and senile changes of varying degree--a new disease? Clinical Neuropathology

Lashuel HA, Overk CR, Oueslati A, Masliah E (2013) The many faces of α-synuclein: from structure and toxicity to therapeutic target. Nat Rev Neurosci 14:38–48. https://doi.org/10.1038/nrn3406

Lashuel HA, Petre BM, Wall J, *et al* (2002) α-Synuclein, Especially the Parkinson's Disease-associated Mutants, Forms Pore-like Annular and Tubular Protofibrils. J Mol Biol 322:1089–1102. https://doi.org/10.1016/s0022-2836(02)00735-0

Lee J-G, Takahama S, Zhang G, *et al* (2016) Unconventional secretion of misfolded proteins promotes adaptation to proteasome dysfunction in mammalian cells. Nat Cell Biol 18:765–776. https://doi.org/10.1038/ncb3372

Lee YW, Kim DH, Jeon SJ, *et al* (2013) Neuroprotective effects of salvianolic acid B on an Aβ25–35 peptide-induced mouse model of Alzheimer's disease. Eur J Pharmacol 704:70–77. https://doi.org/10.1016/j.ejphar.2013.02.015

LEWY F (1912) Paralysis agitans. I. Pathologische Anatomie Handbuch der Neurologie

Li J-Y, Englund E, Holton JL, *et al* (2008) Lewy bodies in grafted neurons in subjects with Parkinson's disease suggest host-to-graft disease propagation. Nat Med 14:501–503. https://doi.org/10.1038/nm1746

Litvan I, MacIntyre A, Goetz CG, *et al* (1998) Accuracy of the Clinical Diagnoses of Lewy Body Disease, Parkinson Disease, and Dementia With Lewy Bodies: A Clinicopathologic Study. Arch Neurol-chicago 55:969–978. https://doi.org/10.1001/archneur.55.7.969

Lloyd KG, Davidson L, Hornykiewicz O (1975) The neurochemistry of Parkinson's disease: effect of L-dopa therapy. J Pharmacol Exp Ther 195:453–64

Luk KC, Kehm V, Carroll J, *et al* (2012) Pathological α-Synuclein Transmission Initiates Parkinson-like Neurodegeneration in Nontransgenic Mice. Science 338:949–953. https://doi.org/10.1126/science.1227157

Ma J, Wang F (2014) Prion disease and the 'protein-only hypothesis.' Essays Biochem 56:181–191. https://doi.org/10.1042/bse0560181

Macosko EZ, Basu A, Satija R, *et al* (2015) Highly Parallel Genome-wide Expression Profiling of Individual Cells Using Nanoliter Droplets. Cell 161:1202–1214. https://doi.org/10.1016/j.cell.2015.05.002

Malta CD, Cinque L, Settembre C (2019) Transcriptional Regulation of Autophagy: Mechanisms and Diseases. Frontiers Cell Dev Biology 7:114. https://doi.org/10.3389/fcell.2019.00114

Mao X, Ou MT, Karuppagounder SS, *et al* (2016) Pathological α-synuclein transmission initiated by binding lymphocyte-activation gene 3. Science 353:aah3374. https://doi.org/10.1126/science.aah3374

Marmion DJ, Peelaerts W, Kordower JH (2021) A historical review of multiple system atrophy with a critical appraisal of cellular and animal models. J Neural Transm 128:1507–1527. https://doi.org/10.1007/s00702-021-02419-8

Martí MJ, Tolosa E, Campdelacreu J (2003) Clinical overview of the synucleinopathies. Movement Disord 18:21–27. https://doi.org/10.1002/mds.10559

Marui W, Iseki E, Nakai T, *et al* (2002) Progression and staging of Lewy pathology in brains from patients with dementia with Lewy bodies. J Neurol Sci 195:153–159. https://doi.org/10.1016/s0022-510x(02)00006-0

McKeith IG, Boeve BF, Dickson DW, *et al* (2017) Diagnosis and management of dementia with Lewy bodies: Fourth consensus report of the DLB Consortium. Neurology 89:88–100. https://doi.org/10.1212/wnl.0000000000004058

McLean PJ, Kawamata H, Hyman BT (2001) α-Synuclein–enhanced green fluorescent protein fusion proteins form proteasome sensitive inclusions in primary neurons. Neuroscience 104:901–912. https://doi.org/10.1016/s0306-4522(01)00113-0

Moreau A-S, Jia X, Ngo HT, *et al* (2007) Protein kinase C inhibitor enzastaurin induces *in vitro* and *in vivo* antitumor activity in Waldenström macroglobulinemia. Blood

109:4964–4972. https://doi.org/10.1182/blood-2006-10-054577

Nalls MA, Blauwendraat C, Vallerga CL, *et al* (2019) Identification of novel risk loci, causal insights, and heritable risk for Parkinson's disease: a meta-analysis of genome-wide association studies. Lancet Neurology 18:1091–1102. https://doi.org/10.1016/s1474-4422(19)30320-5

Nuber S, Rajsombath M, Minakaki G, *et al* (2018) Abrogating Native α-Synuclein Tetramers in Mice Causes a L-DOPA-Responsive Motor Syndrome Closely Resembling Parkinson's Disease. Neuron 100:75-90.e5. https://doi.org/10.1016/j.neuron.2018.09.014

Olanow CW, Perl DP, DeMartino GN, McNaught KSP (2004) Lewy-body formation is an aggresome-related process: a hypothesis. Lancet Neurology 3:496–503. https://doi.org/10.1016/s1474-4422(04)00827-0

Palmieri M, Impey S, Kang H, *et al* (2011) Characterization of the CLEAR network reveals an integrated control of cellular clearance pathways. Hum Mol Genet 20:3852–3866. https://doi.org/10.1093/hmg/ddr306

Parkinson J (1817) An Essay on the Shaking Palsy

Paumier KL, Luk KC, Manfredsson FP, *et al* (2015) Intrastriatal injection of pre-formed mouse α-synuclein fibrils into rats triggers α-synuclein pathology and bilateral nigrostriatal degeneration. Neurobiol Dis 82:185–199. https://doi.org/10.1016/j.nbd.2015.06.003

Peelaerts W, Bousset L, Perren AV der, *et al* (2015) α-Synuclein strains cause distinct synucleinopathies after local and systemic administration. Nature 522:340–344. https://doi.org/10.1038/nature14547

Peng C, Gathagan RJ, Covell DJ, *et al* (2018) Cellular milieu imparts distinct pathological α-synuclein strains in α-synucleinopathies. Nature 557:558–563. https://doi.org/10.1038/s41586-018-0104-4

Polymeropoulos MH, Lavedan C, Leroy E, *et al* (1997) Mutation in the α-Synuclein Gene Identified in Families with Parkinson's Disease. Science 276:2045–2047. https://doi.org/10.1126/science.276.5321.2045

Postuma RB, Aarsland D, Barone P, *et al* (2012) Identifying prodromal Parkinson's disease: Pre-Motor disorders in Parkinson's disease. Movement Disord 27:617–626. https://doi.org/10.1002/mds.24996

Prusiner SB, Woerman AL, Mordes DA, *et al* (2015) Evidence for α-synuclein prions causing multiple system atrophy in humans with parkinsonism. Proc National Acad Sci 112:E5308–E5317. https://doi.org/10.1073/pnas.1514475112

Ren Z, Zhao Y, Cao T, Zhen X (2016) Dihydromyricetin protects neurons in an MPTP-induced model of Parkinson's disease by suppressing glycogen synthase kinase-3 beta activity. Acta Pharmacol Sin 37:1315–1324. https://doi.org/10.1038/aps.2016.42

Rey NL, George S, Steiner JA, *et al* (2018) Spread of aggregates after olfactory bulb injection of α-synuclein fibrils is associated with early neuronal loss and is reduced long term. Acta Neuropathol 135:65–83. https://doi.org/10.1007/s00401-017-1792-9

Rey NL, Petit GH, Bousset L, *et al* (2013) Transfer of human α-synuclein from the olfactory bulb to interconnected brain regions in mice. Acta Neuropathol 126:555–573. https://doi.org/10.1007/s00401-013-1160-3

Reyes JF, Olsson TT, Lamberts JT, *et al* (2015) A cell culture model for monitoring α-synuclein cell-to-cell transfer. Neurobiol Dis 77:266–275. https://doi.org/10.1016/j.nbd.2014.07.003

Sanders DW, Kaufman SK, DeVos SL, *et al* (2014) Distinct Tau Prion Strains Propagate in Cells and Mice and Define Different Tauopathies. Neuron 82:1271–1288. https://doi.org/10.1016/j.neuron.2014.04.047

Sanjana NE, Shalem O, Zhang F (2014) Improved vectors and genome-wide libraries for CRISPR screening. Nat Methods 11:783–784. https://doi.org/10.1038/nmeth.3047

Savage SR, Zhang B (2020) Using phosphoproteomics data to understand cellular signaling: a comprehensive guide to bioinformatics resources. Clin Proteom 17:27. https://doi.org/10.1186/s12014-020-09290-x

Schober A (2004) Classic toxin-induced animal models of Parkinson's disease: 6-OHDA and MPTP. Cell Tissue Res 318:215–224. https://doi.org/10.1007/s00441-004-0938-y

Schrag A, Ben-Shlomo Y, Quinn N (1999) Prevalence of progressive supranuclear palsy and multiple system atrophy: a cross-sectional study. Lancet 354:1771–1775. https://doi.org/10.1016/s0140-6736(99)04137-9

Settembre C, Malta CD, Polito VA, *et al* (2011) TFEB Links Autophagy to Lysosomal Biogenesis. Science 332:1429–1433. https://doi.org/10.1126/science.1204592

Shalem O, Sanjana NE, Hartenian E, *et al* (2014) Genome-Scale CRISPR-Cas9 Knockout Screening in Human Cells. Science 343:84–87. https://doi.org/10.1126/science.1247005

Shulman JM, Jager PLD, Feany MB (2011) Parkinson's Disease: Genetics and Pathogenesis. Pathology Mech Dis 6:193–222. https://doi.org/10.1146/annurev-pathol-011110-130242

Si X, Tian J, Chen Y, *et al* (2019) Central Nervous System-Derived Exosomal α-Synuclein in Serum May Be a Biomarker in Parkinson's Disease. Neuroscience 413:308–316. https://doi.org/10.1016/j.neuroscience.2019.05.015

Simola N, Morelli M, Carta AR (2007) The 6-Hydroxydopamine model of parkinson's disease. Neurotox Res 11:151–167. https://doi.org/10.1007/bf03033565

Spillantini MG, Schmidt ML, Lee VM-Y, *et al* (1997) α-Synuclein in Lewy bodies. Nature 388:839–840. https://doi.org/10.1038/42166

Stoker TB, Greenland JC (2018) Parkinson's Disease Pathogenesis and Clinical Aspects. Australia

Stopschinski BE, Diamond MI (2017) The prion model for progression and diversity of neurodegenerative diseases. Lancet Neurology 16:323–332. https://doi.org/10.1016/s1474-4422(17)30037-6

Svanbergsson A, Ek F, Martinsson I, *et al* (2021) FRET-Based Screening Identifies p38 MAPK and PKC Inhibition as Targets for Prevention of Seeded α-Synuclein Aggregation. Neurotherapeutics 1–18. https://doi.org/10.1007/s13311-021-01070-1

Tenreiro S, Reimão-Pinto MM, Antas P, *et al* (2014) Phosphorylation Modulates Clearance of α-Synuclein Inclusions in a Yeast Model of Parkinson's Disease. Plos Genet 10:e1004302. https://doi.org/10.1371/journal.pgen.1004302

Tozzi A, Iure A de, Bagetta V, *et al* (2016) α-Synuclein Produces Early Behavioral Alterations via Striatal Cholinergic Synaptic Dysfunction by Interacting With GluN2D N-Methyl-D-Aspartate Receptor Subunit. Biol Psychiat 79:402–414. https://doi.org/10.1016/j.biopsych.2015.08.013

Volpicelli-Daley LA, Luk KC, Patel TP, *et al* (2011) Exogenous α-Synuclein Fibrils Induce Lewy Body Pathology Leading to Synaptic Dysfunction and Neuron Death. Neuron 72:57–71. https://doi.org/10.1016/j.neuron.2011.08.033

Walusinski O (2018) Jean-Martin Charcot and Parkinson's disease: Teaching and teaching materials. Rev Neurol 174:491–505. https://doi.org/10.1016/j.neurol.2017.08.005

Wenning GK, Shlomo YB, Magalhães M, *et al* (1994) Clinical features and natural history of multiple system atrophy: An analysis of 100 cases. Brain 117:835–845. https://doi.org/10.1093/brain/117.4.835

Willingham S, Outeiro TF, DeVit MJ, *et al* (2003) Yeast Genes That Enhance the Toxicity of a Mutant Huntingtin Fragment or α-Synuclein. Science 302:1769–1772. https://doi.org/10.1126/science.1090389

Woerman AL, Oehler A, Kazmi SA, *et al* (2019) Multiple system atrophy prions retain strain specificity after serial propagation in two different Tg(SNCA*A53T) mouse lines. Acta Neuropathol 137:437–454. https://doi.org/10.1007/s00401-019-01959-4

Wood SJ, Wypych J, Steavenson S, *et al* (1999) α-Synuclein Fibrillogenesis Is Nucleation-dependent IMPLICATIONS FOR THE PATHOGENESIS OF PARKINSON'S DISEASE*. J Biol Chem 274:19509–19512. https://doi.org/10.1074/jbc.274.28.19509

Yamasaki TR, Holmes BB, Furman JL, *et al* (2019) Parkinson's disease and multiple

system atrophy have distinct α-synuclein seed characteristics. J Biol Chem 294:1045–1058. https://doi.org/10.1074/jbc.ra118.004471

Zabrocki P, Pellens K, Vanhelmont T, *et al* (2005) Characterization of α-synuclein aggregation and synergistic toxicity with protein tau in yeast. Febs J 272:1386–1400. https://doi.org/10.1111/j.1742-4658.2005.04571.x

Zhang W, Tarutani A, Newell KL, *et al* (2020) Novel tau filament fold in corticobasal degeneration. Nature 580:283–287. https://doi.org/10.1038/s41586-020-2043-0

Zhou J, Ruggeri FS, Zimmermann MR, *et al* (2020) Effects of sedimentation, microgravity, hydrodynamic mixing and air–water interface on α-synuclein amyloid formation. https://pubs.rsc.org/en/content/articlepdf/2020/sc/d0sc00281j. Accessed 31 Oct 2021

Acknowledgements

It's a strange feeling to have come to the end of this project. Basically, it has seemed like a destination that was so far off in the distance for the majority of the way until suddenly, it was right there at the doorstep. While at this point it seems like the time has rushed past, I will have to admit that I have experienced a lot, and it is the people I have gotten to share this with as well as those that have made it possible, I want to give my gratitude to.

First, I want to thank my supervisor **Jia-Yi**, for giving me the opportunity to take on this project. I know it has not always been easy to keep me focused on just one project when there was always so many that were interesting. But at the same time I want to thank you deeply for giving me the freedom to pursue ideas and develop the independence needed to run projects. I have learned a lot, and while there are still many things I would like to learn from you, I hope it will be possible to come back and ask you for guidance.

While I have spent the majority of my time in A10, I actually started out my time in Lund at B11. Starting out in a new place not knowing anyone can always seem a little frightening. Luckily, I quickly meet people who welcomed me and made all the long days spend at the BMC a lot more fun. Among the first friends I met over here I really wanted to thank **Nadja, Isak, Jonatan and Emelie**. To this day, I still miss the board game evenings we used to have in the B11 kitchen.

From the early days in A10, I want to say thanks to **Patrick** for always making the days interesting with good banter and conversations that always veered off into strange directions. Also, I want that MtG rematch… And **Carla**, the best almost neighbour for 2 years if I can count. Thank you, for the dinners and good company, which by the way are missed here in Lund ever since you skipped over to Cph!

The importance of having a good work environment does shine through after 5-6 years in one place. And for helping making it so, I really wanted to thank you all: **Elna, Kajsa, Filip, Jana, Sara, Francesco, Janitha, Robert** and **Andreas E**. Also I know we have slacked a bit off on fika, but hopefully that can be brought back now that things are returning to normal.

To the group, **Laura TG, Edo** and **Caroline,** I want to thank you for the support that you have provided. For the number of projects we have conducted and concocted, we really have been busy. We are really going into an interesting time with

graduations coming up for almost all of us. While it is my time now, I look forward to attending your defences in the time to come.

As life needs energy, colour and excitement, there certainly have been a lot of everything at any and all gatherings of yours **Fabio, Eliska, Carolina, Julie, Locko, Marija, Jessica, Roberta** and the rest of the Festive people.

For a lot of funny/random little conversations, **Andreas B.** While I have had a tendency to go on walks around the BMC, I think you take the price with all the traversing of the entire A and B house you have to do going from lab to lab.

Now to some of the most interesting scientific discussions as a part of the MnM Journal club, which I have been very grateful for. So, thank you **Marcus** for dragging me along that once that turned to a regular occurance, and **Tomas** for allowing me to attend on the regular. I also wanted to thank you for taking on the role of guiding my endeavours in the world of the molecular. Your guidance has been invaluable to me.

Marcus & Andi, two guys without whom I would likely have drifted off course a long time ago and gotten lost somewhere in the sea of projects and other fun stuff that seems to attract my attention. Having had you as guides, that have sailed the waters that I know little about. Though I still don't understand why you kept building so many fires.

Its seldom I come across someone with as much overlap in interests as you **Luis**. Having been able to exchange notes on reading material, both scientific and otherwise, I hope we can keep up that exchange.

There exists a number of important life skills to learn, such as budgeting, critical thinking, flow cytometry and live-cell imaging. Interestingly, I think I have picked up all of those up with you **Anna H**. I wanted to thank you for helping me become confident and capable of running what may be two of the most important methods for me through this project. That and learning to think about the costs of running live-cell experiments before running a 7 day, all-out acquisition.

To the most wonderful of people, my support network here in Sweden and dear friends. **Laura**, while I still have to educate you on the finer joys in life (Magic cards and miniatures), I want to thank you for the little pep-talks we always end up having when as I pass by your corridor. Keep practicing those dance moves as the centrifuge spins! It brings joy. **Marta** and **Oscar**, to the loveliest couple. Thank you for all the good moments we have had with dinners and good company at yours. I am looking forward to the next Eurovision as that has become a highlight of the year to celebrate with you. **Martina**, you do realize that now that you are in Vienna I am left deprived of hot chocolate companions and afternoon talks. I do seriously think you need to look into coming back to Lund! Otherwise, I will have to make it

to Vienna next time, as I miss you back here. **Kat**, for all the wonderful dinners and deep talks and strange uber rides over small distances in Lund. Also I still believe you may have a backup career in working with cells if you want to make the switch at some point. **Matilde**, while I have stopped by your office frequently for coffee, it is as much the company that I come for. Whenever things are upsetting, you are always good for putting things in perspective and and lightening up the mood. Especially helping over the last month keeping me grounded has been a world of help. **Martino**, you are a constant source of motivation and confidence. You always seem to have confidence in me even when I dont have any myself! **Lavanya**, our best travel guide, and connoisseur of all the finer things in life. It has been a while since we have had dinners and movies, but considering the list of Marvel movies we are still missing, i thing we need to pick up the pace! **Myriam**, for the little everything's. For inviting over for cosy little get togethers and chilling in Kämnärs. There is never any doubt that when things are hectic you are always there with a helping hand. **Ana**, I am sure I dont know anyone that can surpass you in energy! The best thing about that is that it radiates and lifts up everyone around. **Jordi, Mo**, I do believe I owe you a golf trip! We are slowly getting into the same period again but maybe we will actually make it this time. **Sid** and **Tabor**, we also have some unfinished business, in the shape of a little bottle of undrinkable, ulcer-inducing snaps. Maybe we can take it up over a game of Magic when we get started on it.

Til vennerne hjemmefra **Martin, Mia, Kai, Peter, Leaf, Tjavs, Rene, Bugge, Laura, Bjørn** og **Ask**. Selvom jeg efterhåenden har været væk hjemme fra i en lang periode, har jeg altid følt at jeg har jer med mig. I er blandt mine nærmeste og det synes jeg skulle siges. Jeg håber at jeg nu får lidt mere plads i kalenderen når jeg nu er færdig med den her afhandling så jeg kan komme og være mere med der hjemme.

Maria, I can't say how much your support through this all means to me. You have helped keep me sane through it all, and made sure I actually made it through. While you may think you have been blunt at points, being able to get an answer straight as you see it is invaluable to me. Now that the thesis work is winding down, I think it will be my time to finally give back, and hopefully we can finally go traveling a bit.

Til min kæreste **forældre**, lille søster **Anna** og **Mormor** og **Morfar** vil jeg holde det kort og bare sige at have jer i mit liv betyder alt verden for mig. I er dem der star mit hjærte nærest, og selvom jeg ikke altid er god til at sætte ord til det håber jeg at jeg formår at vise det. En speciel tak går også til min fantastisk onkel **Steffen** som altid står klar hvis der er behov, og som nu har været med hele vejen fra kandidat forsvar til PhD.

Det er til jer alle at jeg dedikere denne afhandling.